THE JOURNAL OF BIOLOGICAL CHEMISTRY VOL. 290, NO. 7, pp. 3910–3924, February 13, 2015
Published in the U.S.A.

Osteoblast Menin Regulates Bone Mass *in Vivo*[*]

Received for publication, December 3, 2014 Published, JBC Papers in Press, December 23, 2014, DOI 10.1074/jbc.M114.629899

Ippei Kanazawa[‡1,2], Lucie Canaff[‡1], Jad Abi Rafeh[§3], Aarti Angrula[‡], Jingjing Li[¶], Ryan C. Riddle[‖], Iris Boraschi-Diaz[¶4], Svetlana V. Komarova[¶], Thomas L. Clemens[‖**], Monzur Murshed[‡¶], and Geoffrey N. Hendy[‡§‡‡§§¶¶5]**

From the Departments of [‡]Medicine, [§]Physiology, [‡‡]Human Genetics, and [¶]Dentistry, [§§]Calcium Research Laboratory, and [¶¶]Hormones and Cancer Research Unit, Royal Victoria Hospital, McGill University, Montreal, Quebec H3A 1A1, Canada, [‖]Department of Orthopaedic Surgery, Johns Hopkins University School of Medicine, Baltimore, Maryland 21205, and the [**]Veterans Administration Medical Center, Baltimore, Maryland 21201

Background: Constitutive homozygous *Men1*$^{-/-}$ mice at mid-gestation are small with craniofacial defects.
Results: Conditional osteoblast *Men1* knock-out mice have reduced bone mass, and transgenic osteoblast menin-overexpressing mice have increased bone mass.
Conclusion: Knock-out mice menin-deficient primary osteoblasts have impaired mineralization and reduced responsiveness to TGF-β and BMP-2.
Significance: Menin is a potential target for gain of function therapeutics in low bone mass disorders.

Menin, the product of the multiple endocrine neoplasia type 1 (*Men1*) tumor suppressor gene, mediates the cell proliferation and differentiation actions of transforming growth factor-β (TGF-β) ligand family members. *In vitro*, menin modulates osteoblastogenesis and osteoblast differentiation promoted and sustained by bone morphogenetic protein-2 (BMP-2) and TGF-β, respectively. To examine the *in vivo* function of menin in bone, we conditionally inactivated *Men1* in mature osteoblasts by crossing osteocalcin (OC)-Cre mice with floxed *Men1* (*Men1*$^{f/f}$) mice to generate mice lacking menin in differentiating osteoblasts (OC-*Cre;Men1*$^{f/f}$ mice). These mice displayed significant reduction in bone mineral density, trabecular bone volume, and cortical bone thickness compared with control littermates. Osteoblast and osteoclast number as well as mineral apposition rate were significantly reduced, whereas osteocyte number was increased. Primary calvarial osteoblasts proliferated more quickly but had deficient mineral apposition and alkaline phosphatase activity. Although the mRNA expression of osteoblast marker and cyclin-dependent kinase inhibitor genes were all reduced, that of cyclin-dependent kinase, osteocyte marker, and pro-apoptotic genes were increased in isolated *Men1* knock-out osteoblasts compared with controls. In contrast to the knock-out mice, transgenic mice overexpressing a human menin cDNA in osteoblasts driven by the 2.3-kb *Col1a1* promoter, showed a gain of bone mass relative to control littermates. Osteoblast number and mineral apposition rate were significantly increased in the *Col1a1-Menin-Tg* mice. Therefore, osteoblast menin plays a key role in bone development, remodeling, and maintenance.

Both TGF-β and BMPs,[6] primarily synthesized by osteoblasts, play an important role in bone formation and remodeling (1–3). Autocrine and paracrine stimulation by TGF-β itself is important for the maintenance and expansion of mesenchymal stem cells, the osteoblast progenitors, and is critical for osteoblast differentiation and bone formation. BMPs were initially identified by their ability to induce ectopic bone formation in muscle, and some of them are now approved for use in clinical applications related to long bone fracture repair. Members of the TGF-β ligand superfamily signal through type I and type II serine/threonine kinase cell membrane receptors. The type II receptor is constitutively phosphorylated and, when activated by binding of the ligand, recruits and transphosphorylates the type I receptor. The activated type I receptor phosphorylates the receptor-regulated Smads (R-Smad; Smad2 and Smad3 for TGF-β and Smad1, Smad5, and Smad8 for BMPs) inducing their association with the common partner, Smad4. The R-Smad·Smad4 complex then translocates to the nucleus to activate specific genes (4, 5). The importance of TGF-β and BMPs in many components of the musculoskeletal system has been emphasized by the finding of mutations in their signaling pathway molecules in human skeletal genetic disorders.

[*] This work was supported in part by the Department of Medicine, McGill University Grant 5767 and McGill University Health Centre-Research Institute Grant 5758 (to G. N. H.) and Canadian Institutes of Health Research Grants MOP-9315 (to G. N. H.), 123310 (to M. M.), and 776403 (to S. V. K.).
[1] Both authors contributed equally to this work.
[2] Recipient of fellowships from Fonds de la Recherché en Santé Quebec, Canadian Bureau for International Education, Uehara Memorial Foundation, and Kanae Foundation for the Promotion of Medical Science. Present address: Internal Medicine 1, Shimane University Faculty of Medicine, Izumo, Shimane 693-8501, Japan.
[3] Recipient of a Network for Oral and Bone Health Research (RSBO) Summer Student Scholarship.
[4] Supported by the McGill University Faculty of Dentistry.
[5] To whom correspondence should be addressed: Calcium Research Laboratory, Rm. H4.67, Royal Victoria Hospital, 687 Pine Ave. West, Montreal, Quebec H3A 1A1, Canada. Tel.: 514-843-1632; Fax: 514-843-1712; E-mail: geoffrey.hendy@mcgill.ca.

[6] The abbreviations used are: BMP, bone morphogenetic protein; MEN1, multiple endocrine neoplasia type 1; OC, osteocalcin; Col1a1, type 1 collagen α1; *Men1*$^{f/f}$, floxed *Men1*; *OC-Cre;Men1*$^{f/f}$, osteoblast *Men1* knock-out; *Col1a1-Menin-Tg*, osteoblast Menin overexpressing transgenic; BV, bone volume; TV, tissue volume, BS, bone surface; MS, mineralizing surface; MAR, mineral apposition rate; BMD, bone mineral density; CT, computed tomography; αMEM, α-minimal essential medium; TRAP, tartrate-resistant acid phosphatase; MTT, methyl thiazolyl tetrazolium; ALP, alkaline phosphatase.

The protein menin came to attention initially as the tumor suppressor encoded by the *MEN1* gene that is implicated in the autosomal dominant multiple endocrine neoplasia type 1 (MEN1) disorder. In this syndrome tumors arise in select endocrine (and non-endocrine) tissues during the lifetime of an individual carrying a germ line *MEN1* mutation (6, 7). Menin, a predominantly nuclear protein (8, 9), is widely expressed from early in fetal development onwards. Several strains of *Men1* knock-out mice have been generated, both constitutive and conditional in specific tissues. Heterozygous $Men1^{+/-}$ mice from about 9 months of age develop hyperplasia and tumors of parathyroid and anterior pituitary glands and pancreatic islets (10–12). This mouse model closely mimics human MEN1. Tissue-specific knockouts of the *Men1* gene have been generated in which null expression of *Men1* in parathyroids, the pituitary, and pancreatic islet β-cells has been achieved (13–16). These studies suggest that although loss of menin contributes to the neoplasias that eventually arise, it does not affect normal development in these particular tissues.

Mice that are constitutively homozygous null for the *Men1* gene die *in utero* at mid-gestation of multiple defects in developing organs, suggesting that menin does play critical essential roles in tissues additional to those affected in the MEN1 syndrome (10, 17, 18). The fetuses are small and exhibit craniofacial defects, suggesting that menin might play a role in both endochondral and intramembranous bone formation (10, 17). We previously showed that menin is required for the commitment of multipotential mesenchymal stem cells *in vitro* to the osteoblast lineage (19). This occurs in part by menin facilitating BMP-2 signaling via Smads and the transcriptional activity of the key osteoblast transcription factor, Runx2 (20). Menin interacts physically and functionally with Smads1/5 and Runx2 in mesenchymal stem cells (20). In committed osteoblasts these interactions are for the most part lost, as menin then acts to maintain the osteoblast in its differentiated state. This is mediated in part by menin's interaction with the TGF-β/Smad3 pathway (20, 21).

Based on our previous *in vitro* studies, we hypothesized that menin plays a critical role not only in osteoblastogenesis and osteoblast differentiation but also in bone mass accumulation *in vivo* (22). To further understand the role of menin in bone development *in vivo* we generated and examined mouse models in which the expression of the *Men1* gene is specifically altered only in mature osteoblasts.

EXPERIMENTAL PROCEDURES

Generation of Knock-out and Transgenic Mice

Conditional knock-out and transgenic mouse models in which either the *Men1* gene is deleted or the menin cDNA is overexpressed specifically in differentiated osteoblasts were generated. Mice were maintained in a pathogen-free standard animal facility, and experimental procedures were performed following an animal use protocol approved by the Animal Care and Use Committee of McGill University.

Men1 Knock-out Mice

$Men1^{flox/flox}$ mice were obtained from The Jackson Laboratory (129S(FVB)-$Men1^{tm1.2Ctre}$/J) (10), and *Osteocalcin*-Cre transgenic ($OC\text{-}Cre^{TG/+}$) mice express Cre recombinase with high specificity and penetrance in mature osteoblasts (23). $Men1^{flox/flox}$ mice were crossed with $OC\text{-}Cre^{TG/+}$ mice to generate $OC\text{-}Cre^{TG/+}$;$Men1^{flox/+}$ mice. These mice were crossed with $Men1^{flox/flox}$ mice to generate litters that contained ~¼ $OC\text{-}Cre^{TG/+}$;$Men1^{flox/flox}$ mice, which were used for subsequent crosses. The control littermate mice are designated as $Men1^{f/f}$ and the knock-out mice as *OC-Cre;*$Men1^{f/f}$. Both were on the FVB background.

Col1a1-Menin-Tg Transgenic mice

A full-length FLAG-tagged human menin cDNA preceded by a rabbit β-globin intron was inserted in between a 2.3-kb mouse *Col1a1* promoter fragment (24) and a SV40 polyadenylation signal. The transgene sequence was released from the plasmid backbone by SacII restriction enzyme digestion. Transgenic founders were generated by pronuclear injections at McGill Cancer Center Transgenic Core Facility. For osteoblast-specific menin transgenic mice analysis, their wild-type littermate mice were used as controls. The mutant mouse strain of *Col1a1-Menin-Tg* mice was on the C57BL6/J background.

Osteoblast-specific Men1 Knock-out and Menin-overexpressing Transgenic Mice

Genotyping strategies are available upon request.

OC-Cre;Men1$^{f/f}$ Mice

To test for the specific deletion of *Men1* exons 3–8, genomic DNA isolated from different tissues was amplified using a combination of primers A, C, and D. Primer A (5′-CCCACATCCAGTCCCTCTTCAGCT-3′) is specific to exon 2 of the *Men1* gene. Primer C (5′-CGGAGAAAGAGGTAATGAAATGGC-3′) is specific for the inserted LoxP sequence. Primer D (5′-CATAAAATCGCAGCAGGTGGGCAA-3′) is specific for *Men1* exon 9. PCR of the recombinant Δ3–8 *Men1* allele generates a 638-bp amplicon (primers A + D), and the $Men1^{flox}$ allele generates a 239-bp amplicon (primers A + C).

Col1a1-Menin-Tg Mice

The *OC-Cre* transgene was detected using the primers 5′-CAAATAGCCCTGGCAGATTC-3′ and 5′-TGATACAAGGGACATCTTCC-3′ to generate a 260-bp product corresponding to a portion of the OC promoter and the rabbit β-globin intron.

Reverse transcription (RT)-polymerase chain reaction (PCR) was performed to detect the expression of the *Col1a1-Menin* transgene in tissues. See "Gene Expression Analysis" below for RNA extraction and cDNA synthesis. A forward primer specific for human menin (5′-GTGAGAAGATGAAGGGCATGA-3′) and a reverse primer specific for the SV40 polyadenylation signal (5′-TAATGTGGCTATGGGAATTGGA-3′) amplified a 640-bp transgene product. As an internal standard, a 350-bp product of the hypoxanthine phosphoribosyltransferase (HPRT) cDNA was amplified using specific primers; F (5′-GTTGAGAGATCATCTCCACC-3′) and R (5′-AGCGATGATGAACCAGGTTA-3′). The PCR conditions were 95 °C for 30 s, 60 °C for 30 s, and 72 °C for 1 min for 30 cycles.

Immunoblotting

Tissues and isolated primary osteoblasts were homogenized on ice in triple detergent buffer, and Western blotting was performed as previously described (25) with anti-menin polyclonal antibody, Ab2605 (Abcam), or anti-FLAG M2 antibody (Sigma). Membranes were reprobed with a β-tubulin antibody (Santa Cruz) as the loading control.

Bone Mineral Density (BMD) Analysis by Dual Energy X-ray Absorptiometry

Anesthetized mice were placed prone on a specimen tray in a PIXImus densitometer (Lunar Corp., Madison, WI), densitometry was performed on the right femur, and BMD was calculated with the manufacturer's software (version 1.46.007).

Micro-computed Tomography (Micro-CT)

Mice femurs, dissected free of soft tissue, were fixed overnight in 70% ethanol. High resolution images of the distal femur were acquired with a desktop microtomographic imaging system (SkyScan 1072, Antwerp, Belgium) in accordance with the recommendations of the American Society of Bone and Mineral Research (26). Three-dimensional renderings of the distal 3.5 mm of the femora were reconstructed using two-dimensional data from scanned slices with the 3D creator software (Skyscan). The trabecular bone region of interest was drawn to include all cancellous bone in the metaphysis.

Bone Histomorphometric Analysis

Lumbar vertebrae were dissected, fixed for 24 h in 4% formalin, dehydrated in a graded ethanol series, and embedded in methyl methacrylate resin, and 7-μm sections were made (27). Von Kossa/van Gieson staining was done, and histomorphometric analyses were made with Osteomeasure software (OsteoMetrics Inc.). The parameters comply with the guidelines of the American Society of Bone and Mineral Research nomenclature committee (28). For analysis of osteoblasts, osteocytes, and osteoclasts, 5-μm sections were stained with toluidine blue and tartrate-resistant acid phosphatase, respectively. Images were taken at room temperature using a light microscope (DM200; Leica) with a 20× (numerical aperture of 0.40) or 40× (numerical aperture of 0.65) objective. All histological images were captured using a camera (DP72; Olympus), acquired with DP2-BSW software (XV3.0; Olympus), and processed using Photoshop (Adobe).

TUNEL Assay

To evaluate osteoblast apoptosis the TUNEL assay was performed on undecalcified vertebral sections (see above) using the Deadend Fluorometric TUNEL System kit (Promega). Images were captured on an EVOS FL Digital Inverted Fluorescent Microscope (Fisher).

Double Calcein Labeling

Calcein (Sigma; C-0875) was dissolved in buffer (0.15 M NaCl, 2% $NaHCO_3$) and injected twice intraperitoneally (25 μg/g body weight) at 9 and 2 days before the mice were killed (29). Bones were harvested and embedded in plastic as described above. Serial sections were cut, and the freshly cut surface of each section was viewed and imaged using fluorescence microscopy. The double calcein-labeled width was measured using Osteomeasure software, and the mineral apposition rate (MAR = interlabel width/labeling period), bone formation rate/bone surface (BS), and mineralizing surface (MS)/BS were calculated. Calculations were made on a minimum of duplicate specimens from replicate mice of each group.

Osteoclastogenesis Assay

Bone marrow cells were collected from mouse long bones under aseptic conditions as described previously (30) and were cultured overnight with M-CSF (25 ng/ml Preprotech; 300–25). The following day non-adherent precursors were plated at 5×10^4 cells/cm^2 and treated with M-CSF (50 ng/ml) and recombinant soluble RANKL (50 ng/ml) (31) for 5 days after which osteoclast numbers were quantified (see below).

Osteoclast/Osteoblast Co-culture Assay

Bone marrow cells were plated at 1.5×10^6 cells/cm^2 and cultured in α-minimal essential medium (αMEM, Invitrogen; 12000–022) supplemented with 10% FBS (Wisent; 080152), with 1% sodium pyruvate (Wisent; 600–110-EL), and 1% penicillin-streptomycin (Wisent; 450–201-EL) and 0.02 M sodium bicarbonate (Sigma; S5761–500G). One day after plating, 50 μg/ml L-ascorbic acid (Sigma; A8960–5G) was added to induce osteoblast differentiation. Every other day the medium was changed, and freshly prepared ascorbic acid was added. On day 8, samples were fixed with 10% formalin in PBS, pH 7.4, for 8–9 min at room temperature and stained for alkaline phosphatase (ALP; Fast Red, Sigma; F4381) or tartrate-resistant acid phosphatase (TRAP, Sigma; 387A). For each well five images were taken at pre-defined positions, and the color intensity was analyzed using Image J software (imagej.nih.gov). Osteoclast numbers were quantified by counting TRAP-positive cells with three or more nuclei and intact membrane.

Fluorescence Labeling

Co-cultures on glass coverslips were fixed on day 9 with 10% formalin, permeabilized with 0.1% Triton X-100 (Fisher; BP151-100) in PBS for 10 min, incubated for 20 min at room temperature with a red fluorescent Alexa Fluor 568 tagged phalloidin (Invitrogen; A12380), washed 3 times in PBS and once with distilled water, and incubated with 0.2 μg/ml of 40,6-diamidino-2-phenylindole dihydrochloride (DAPI) in distilled water for 5 min. Slides were washed three times with distilled water and mounted on microscope slides using mounting media (Thermo Scientific; 9990402). Images were recorded using an inverted fluorescence microscope (Eclipse TE2000-U, Nikon) and cooled charge-coupled device camera (Hamamatsu Photonics) supported by Volocity software (Perkin Elmer) (32).

Osteoblast Isolation from Young Mice

Osteoblasts from calvaria of individual 1–2-week-old *OC-Cre;Men1$^{f/f}$* pups or their control littermates were isolated as described (33). The bones were dissected free of sutures and subjected to 2 consecutive digestions at 37 °C with shaking in αMEM medium (Invitrogen) containing 0.1 mg/ml collagenase

P (Roche Applied Science) and 0.25% trypsin/0.1% EDTA (Invitrogen), The supernatant was discarded leaving the pieces of bone. Fresh digestion medium containing 0.2 mg collagenase P/ml was added, and calvaria were incubated at 37 °C with vigorous shaking every 15 min for 45 min or until bone pieces began to fall apart. The bone pieces and cells were collected by centrifugation (1500 × *g*), washed with αMEM, and plated in a 10-cm dish with αMEM containing 10% FBS and 1% penicillin/streptomycin (Invitrogen). After 4 days, the medium was changed, and when the cells reached 80% confluency they were passaged to 6-well plates (10^5 cells/well). After reaching ~70% confluency, the medium was supplemented with 10 mM β-glycerophosphate and 50 μg/μl ascorbic acid (Sigma), and this osteogenic medium was replaced every 3 days.

Osteoblast Isolation from Older Mice

Osteoblasts from calvaria of individual 5–6 month-old *OC-Cre;Men1*$^{f/f}$ mice or their control littermates were isolated as described (34). Calvaria were dissected and transferred to a Petri dish containing PBS, and soft tissues were removed by scraping the bone with a scalpel. Sutures were removed, and the rest of the calvaria was chopped into small fragments. The fragments were incubated for 30 min at 37 °C with shaking in 2 mg of collagenase II/ml αMEM (Bioshop Inc), the supernatant was discarded, and the procedure was repeated. Calvaria were then incubated for 30 min at 37 °C with shaking in a 0.25% trypsin, 0.1% EDTA solution. The supernatant was discarded and replaced by fresh collagenase II solution for the fourth and final incubation step of 30 min at 37 °C. Bone pieces were washed 3 times with αMEM containing 10% FBS and 1% penicillin/streptomycin, 10 mM β-glycerophosphate, and 50 μg/μl ascorbic acid ("osteogenic medium") and transferred to T75 flasks. Medium was changed every 3 days. Adult mouse bone cells migrated from the bone chips after 2–3 days, and after 7 days the cells were passaged to 6-well plates (10^5 cells/well).

Adenovirus Infection of Osteoblasts

Osteoblasts were isolated from calvaria of neonatal and adult *Men1*$^{f/f}$ mice as above. They were grown to 70% confluency and infected with control adenovirus expressing green-fluorescent protein (ad-GFP) or adenovirus expressing Cre recombinase (ad-Cre, Vector Biolabs) at an multiplicity of infection of 100 (35). Forty-eight hours after adenoviral infection, cells were replated for proliferation and differentiation assays.

Gene Expression Analysis in Osteoblasts

For gene expression analyses, RT-PCR was performed. Total RNA was prepared from primary osteoblasts in 6-well plates using the standard TRIzol method as recommended by the manufacturer (Invitrogen) and subjected to DNase I (Invitrogen) treatment. Semiquantitative RT-PCR was performed to estimate the abundance of specific mRNAs relative to GAPDH mRNA. Two μg of total RNA was employed for the synthesis of single-stranded cDNA using a high capacity cDNA reverse transcription kit (Applied Biosystems). Primer sequences and cycle numbers are available on request.

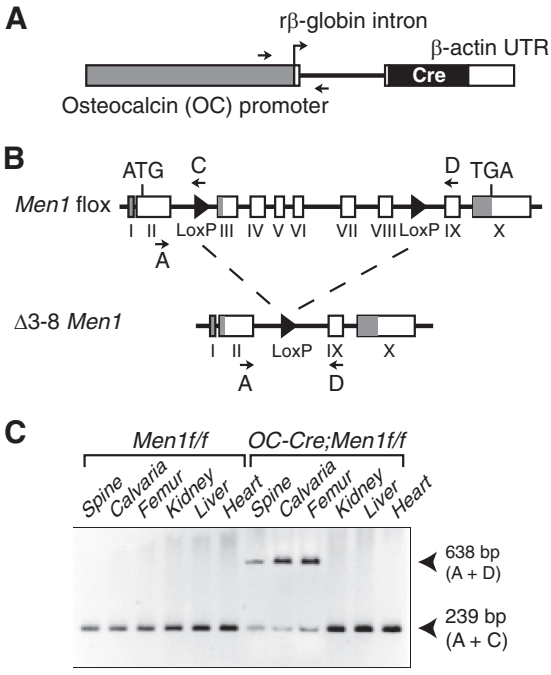

FIGURE 1. **Osteoblast-specific deletion of *Men1* with *OC-Cre*.** *A*, osteoblast-specific osteocalcin promoter driving expression of the Cre recombinase cDNA in the transgene. *B*, the target *Men1*^{flox} and the recombinant Δ3–8 *Men1* alleles. Locations of the genotyping primers (*A*, *C*, and *D*) are indicated (*arrows*). *Filled triangles*, LoxP sites. *C*, genomic DNA from mouse tissues was used as a template for multiplex PCR amplification with primers A + C + D. Product A + D = 638 bp (recombinant Δ3–8 *Men1* allele); product A + C = 239 bp (target *Men1*^{flox} allele). The *Men1* gene deletion is specific for bone.

ALP Activity and Mineral Apposition

Confluent primary cultures of osteoblasts were grown in differentiation osteogenic medium. ALP activity was determined by histochemical staining at days 7–10 post-differentiation using the Fast Red TR/Naphthol AS-MX tablet set (Sigma). Cells were washed with PBS then fixed at room temperature for 10 min using 100% ethanol. After removal of the ethanol, cells were washed with distilled water, and stain was added. Fixed cells were incubated at 37 °C for 30 min then washed with running water and air-dried.

Phosphate deposition was evaluated in osteoblasts 10 days post-differentiation. Osteoblasts were washed with PBS and fixed with 4% paraformaldehyde for 10 min at room temperature. Fixed cells were washed 5 times with distilled water >30 min then stained with von Kossa solution (3% silver nitrate in distilled water) under bright light. Cells were washed before scanning or photographing.

Calcium deposition was determined by alizarin red-S staining. Cells were rinsed with PBS, fixed for 10 min in 100% ethanol at room temperature, washed with distilled water, then stained for 30 min with 4 mM alizarin red-S, pH 4.2. Alizarin red-S was extracted by destaining with 10 mM HCl in 70% ethanol, and mineral accumulation was quantified on a microplate reader at 520 nm. The cell layer was then solubilized in lysis buffer (10 mM formamide, 50 mM sodium acetate, 1% SDS, pH 6), and protein content was assessed by a Bradford assay. Results were calculated as nmol of alizarin red-S/mg of protein and expressed as -fold change *versus* control.

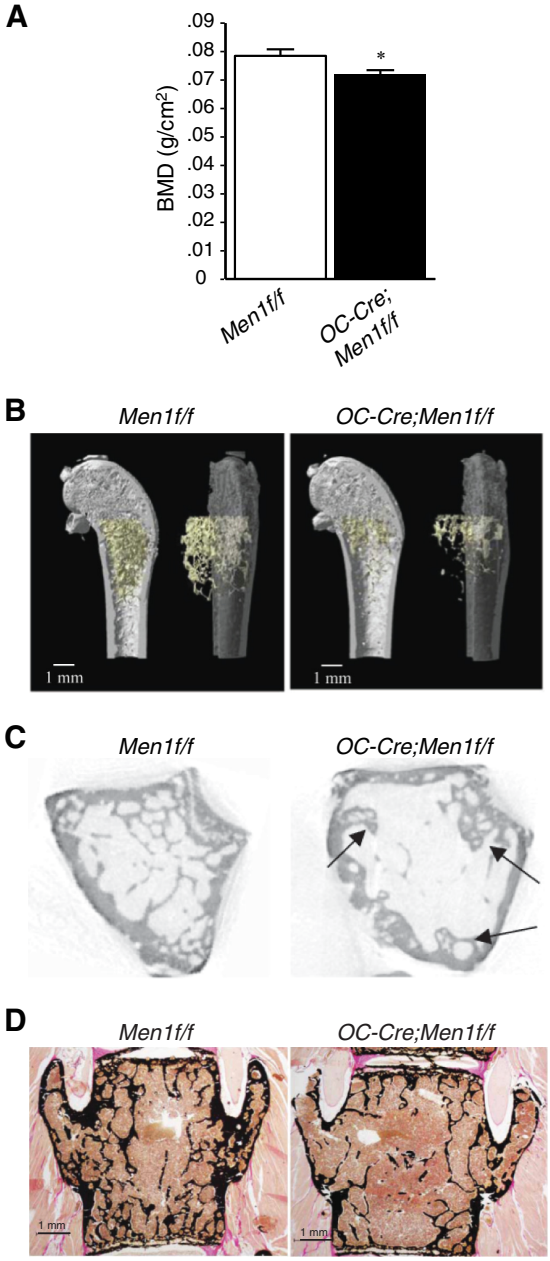

FIGURE 2. **Deletion of osteoblast *Men1* leads to reduction in BMD and decreased bone volume.** *A*, BMD (measured by dual energy x-ray absorptiometry) of femur from 9-month-old *OC-Cre;Men1*$^{f/f}$ ($n = 7$) and control (*Men1*$^{f/f}$) littermate mice ($n = 7$). *B*, micro-CT analysis of distal femur of 9-month-old *OC-Cre;Men1*$^{f/f}$ and control (*Men1*$^{f/f}$) mice (representative images are shown). *C*, trabecular bone was reduced in *OC-Cre;Men1*$^{f/f}$ mice compared with *Men1*$^{f/f}$ controls. *Arrows* indicate abnormal formation of trabeculae. See Table 1 for quantitation. Deletion of osteoblast *Men1* leads to reduction in trabecular bone assessed by histomorphometry. *D*, representative images of von Kossa/van Gieson staining of vertebrae of 9-month-old *OC-Cre;Men1*$^{f/f}$ and *Men1*$^{f/f}$ control mice. See Table 1 for quantitation.

TABLE 1

BMD, three-dimensional micro-CT, and histological analysis of femur and histomorphometric analysis of lumbar spine from 9-month-old female *Men1*$^{f/f}$ and *OC-Cre;Men1*$^{f/f}$ mice

Tb, trabecular number; *TbSp*, trabecular separation; SMI, structure model index; TbTh, trabecular thickness; TbN, trabecular number; CtTh, cortical bone thickness; NS, not significant.

Parameter	*Men1*$^{f/f}$	*OC-Cre;Men1*$^{f/f}$	Significance
BMD (g/cm^2)	0.078 ± 0.002	0.072 ± 0.001	$p < 0.05$
Micro-CT			
BV/TV (%)	5.38 ± 0.74	2.88 ± 0.29	$p < 0.05$
BS/BV (mm^2/mm^3)	99.40 ± 0.71	78.78 ± 5.97	$p < 0.05$
BS/TV (mm^2/mm^3)	5.34 ± 0.71	2.23 ± 0.04	$p < 0.05$
SMI	2.17 ± 0.05	2.48 ± 0.09	$p < 0.05$
TbTh (mm)	0.05 ± 0.003	0.07 ± 0.004	$p < 0.05$
TbN (1/mm)	1.02 ± 0.14	0.43 ± 0.02	$p < 0.05$
TbSp (mm)	0.34 ± 0.02	0.48 ± 0.02	$p < 0.01$
CtTh (mm)	0.24 ± 0.004	0.20 ± 0.01	$p < 0.05$
Histomorphometry			
BV/TV (%)	14.44 ± 1.0	8.35 ± 0.76	$p < 0.01$
BS/TV (mm^2/mm^3)	10.86 ± 1.1	6.58 ± 0.41	$p < 0.01$
BS/BV (mm^2/mm^3)	74.39 ± 3.20	80.14 ± 4.42	NS
TbTh (μm)	27.19 ± 1.18	25.24 ± 1.31	NS

Osteoblast Proliferation

5-Bromo-2-deoxyuridine (BrdU) Assay—Primary osteoblasts were plated on BD Bioscience 8-well culture slides at a density of 1×10^4 cells/ml, cultured for 3 days, then incubated with 10 μM BrdU (Sigma B5002) for 24 h. Cells were fixed with 4% paraformaldehyde and permeabilized with 1% Triton X-100 in PBS. Antigen retrieval was performed by HCl incubations followed by neutralization with borate buffer. Endogenous peroxidase activity was inhibited by 15 min of incubation with 0.3% hydrogen peroxide. Cells were blocked in 1% BSA in PBS for 30 min, then incubated with biotinylated anti-BrdU (1:3000, ABCAM; ab2284) overnight. After washing with 1% BSA in PBS, cells were incubated with streptavidin-HRP (1:2000, ABCAM; ab7403) for 2 h. Development was performed with diaminobenzidine and counterstained with hematoxylin.

Methyl Thiazolyl Tetrazolium (MTT) Dye Viability Assay Primary osteoblasts were seeded at a density of 4×10^4 cells per well in 24-well tissue culture plates and cultured in phenol red-free DMEM-F-12 at 37 °C. Forty-eight hours later MTT was added, and incubation was continued for 4 h. Acid isopropyl alcohol was added, and absorbance was read at 595 nm.

PrestoBlue Cell Viability Assay—Primary osteoblasts were seeded at a density of 4×10^4 cells per well in 24-well tissue culture plates and cultured in DMEM-F-12 at 37 °C. Forty-eight hours later, PrestoBlue reagent was added, and incubation was continued for 20 min. Absorbance was read at 570 nm and normalized to the 600-nm value.

Osteoblast Apoptosis

Mouse C2C12 cells and adult primary osteoblasts (*Men1*$^{f/f}$ or *OC-Cre;Men1*$^{f/f}$) were seeded at a density of 1×10^6 in 60-mm plates. After 48 h cells were treated or not with 1 mM dexamethasone and incubated for a further 24 h. Proteins in cell lysates were separated by SDS-PAGE, transferred to PVDF membranes and Western-blotted overnight at 4 °C with anti-caspase-3 antibody (ABCAM, ab47131) followed by HRP-conjugated secondary antibody. Detection was performed using enhanced chemiluminescence.

Serum Biochemistries

Mouse blood samples were obtained by cardiac puncture, and serum biochemistries were determined by autoanalyzer at the Comparative Medicine Animal Resources Centre of McGill University.

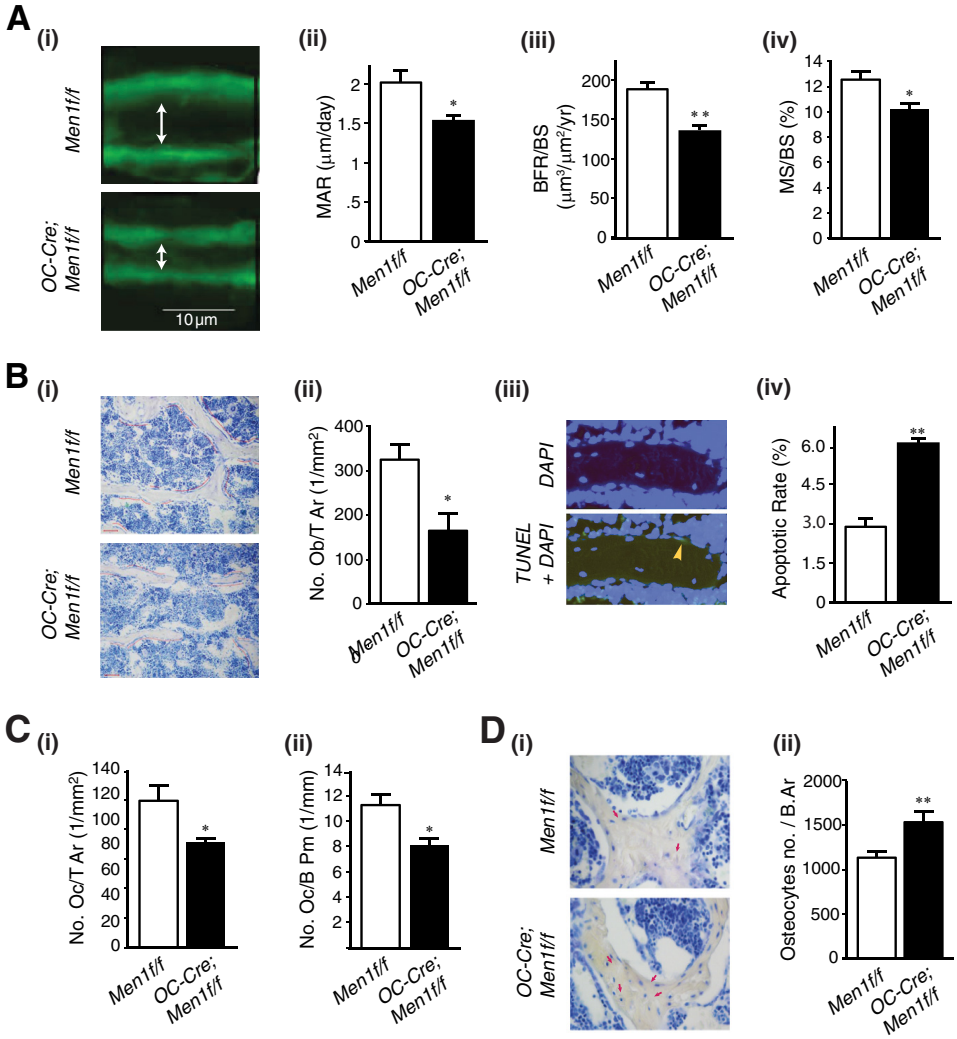

FIGURE 3. **Disruption of *Men1* in osteoblasts impairs bone formation and turnover.** *A*, 9-month-old female mice were labeled with sequential doses of calcein, and dynamic indices of bone formation were quantitated in *OC-Cre;Men1$^{f/f}$* ($n = 3$) and *Men1$^{f/f}$* control ($n = 3$) mice. *i*, representative calcein-labeled sections of vertebrae from *OC-Cre;Men1$^{f/f}$* (*lower panel*) and *Men1$^{f/f}$* control (*upper panel*) mice. MAR (*ii*), bone formation rate/bone surface (*BFR/BS*; *iii*), and MS/BS (*iv*) were all significantly reduced in *OC-Cre;Men1$^{f/f}$* mice relative to controls. *, $p < 0.05$; **, $p < 0.01$. *B*, numbers of osteoblasts were significantly decreased, and their apoptotic rate was increased in *OC-Cre;Men1$^{f/f}$* mice *versus* controls. *i*, representative sections. *ii*, quantitation of osteoblasts, Ob/T Ar. *, $p < 0.05$. *iii*, representative section showing TUNEL staining of osteoblast undergoing apoptosis (*arrow*). *iv*, quantitation of apoptotic osteoblasts. **, $p < 0.01$. *C*, numbers of osteoclasts were significantly decreased in *OC-Cre;Men1$^{f/f}$* mice *versus* controls. *i*, osteoclast tissue area (*Oc/T Ar*). *ii*, osteoclast bone perimeter (*OcB Pm*). *, $p < 0.05$. *D*: *i*, osteocytes (*arrows*) were identified in bone of control *Men1$^{f/f}$* mice (*upper panel*) and osteoblast *Men1* knock-out *OC-Cre;Men1$^{f/f}$* mice (*lower panel*). *ii*, osteocyte number was significantly higher in the *OC-Cre;Men1$^{f/f}$* bone relative to that of *Men1$^{f/f}$* control mice (**, $p < 0.01$).

Statistical Analysis

Results are expressed as the mean ± S.E. Statistical comparisons using GraphPad Prism Version 4.00 analysis software (GraphPad Software, Inc., San Diego, CA) were made using the unpaired two-tailed Student's *t* test, and a *p* value of <0.05 was taken to indicate a significant difference.

RESULTS

Disruption of the Men1 Gene Is Specific to the Bone—PCR amplification of tissue genomic DNA confirmed that *Cre*-mediated recombination occurred specifically in bone of the knock-out, *OC-Cre;Men1$^{f/f}$*, mice (Fig. 1). Body weights (g) (25 ± 1 *versus* 26 ± 0.9), serum levels (mmol/liter) of calcium (2.4 ± 0.1 *versus* 2.4 ± 0.1), phosphate (2.5 ± 0.1 *versus* 2.1 ± 0.2), and magnesium (1.2 ± 0.1 *versus* 1.1 ± 0.1) of *OC-Cre;Men1$^{f/f}$* mice *versus* controls were not different at 9 months of age.

Osteoblast-specific Disruption of the Men1 Gene Decreases Bone Mass and Volume—BMD determined by dual energy x-ray absorptiometry of the femurs of 9-month-old mice was significantly reduced in knock-out mice relative to controls (Fig. 2*A*). *OC-Cre;Men1$^{f/f}$* mice had significant decreases in both trabecular and cortical bone by micro-CT. Trabecular bone volume was markedly reduced in the knock-out mice (Fig. 2*B*), and the trabeculae were of abnormal structure (Fig. 2*C*). Bone volume and surface, trabecular number, and cortical bone thickness were significantly reduced in *OC-Cre;Men1$^{f/f}$* mice (Table 1). Structure model index, trabecular thickness, and trabecular separation were significantly increased (Table 1).

Histomorphometric analysis indicated that trabecular bone volume and surface at lumbar spine was remarkably reduced in *OC-Cre;Men1$^{f/f}$* mice compared with controls (Fig. 2*D*; Table

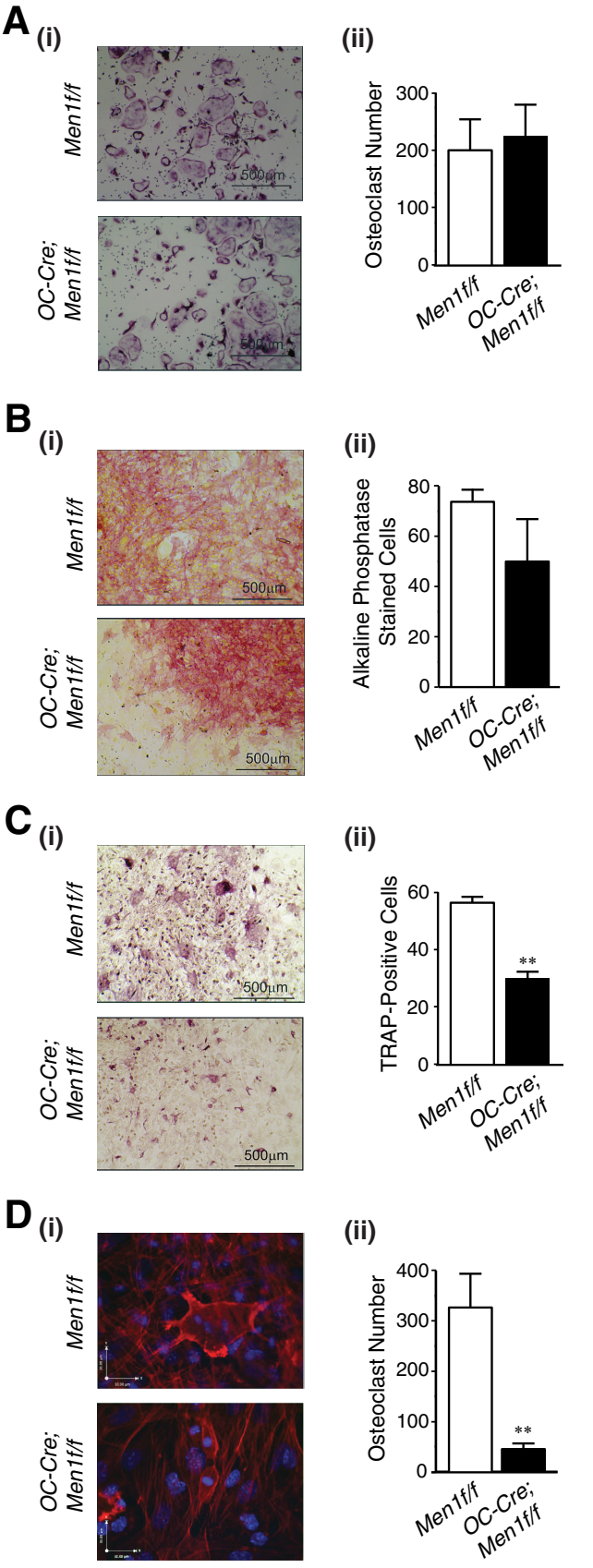

FIGURE 4. **Deletion of *Men1* in osteoblasts leads to decreased support for osteoclastogenesis.** *A*, non-adherent bone marrow osteoclast precursors from six-month-old *OC-Cre;Men1$^{f/f}$* ($n = 8$) and control (*Men1$^{f/f}$*) littermate mice ($n = 7$) were treated with M-CSF (50 ng/ml) and RANKL (50 ng/ml) for 5 days, samples were fixed and stained for TRAP, and osteoclasts were counted. *i*, representative sections. *ii*, quantitation. *B–D*, bone marrow cells from 6-month-old *OC-Cre; Men1$^{f/f}$* ($n = 8$) and control (*Men1$^{f/f}$*) littermate mice ($n = 7$) were plated at 1.5×10^6 cells/cm^2, treated with L-ascorbic acid (50 μg/ml) for 8 days, and fixed. *B*, samples were stained for alkaline phosphatase, and the color intensity was assessed. *i*, representative sections. *ii*, quantitation. *C*, samples were stained for TRAP, and the color intensity was assessed. *i*, representative sections. *ii*, quantitation. **, $p < 0.01$. *D*, samples were stained for actin (*red*) and DNA (DAPI, *blue*). Osteoclasts have characteristic actin ring staining and podosomes in contrast to the actin-stained stress fibers of osteoblasts. *i*, representative sections. *Upper panel*, *Men1$^{f/f}$* control with osteoclast having three nuclei; *lower panel*, *OC-Cre; Men1$^{f/f}$* with two monocytes. *ii*, quantitation of mature osteoclasts having ≥3 nuclei and intact membrane. **, $p < 0.01$.

1). These combined data show that trabecular and cortical bone mass were reduced, and trabecular structure was altered in *OC-Cre;Men1$^{f/f}$* mice.

Deletion of the Men1 Gene in Osteoblasts Decreases Bone Formation and Turnover—Cancellous MAR, bone formation rate/BS, and MS/BS were significantly decreased in *OC-Cre;Men1$^{f/f}$* mice compared with controls (Fig. 3*A*, *i–iv*). In addition, the number of osteoblasts was significantly reduced in *OC-Cre; Men1$^{f/f}$* mice relative to controls (Fig. 3*B*, *i* and *ii*). The apoptotic rate of osteoblasts in the menin knock-out *OC-Cre;Men1$^{f/f}$* mice was increased *versus* control mice assessed by TUNEL assay (Fig. 3*B*, *iii* and *iv*). Moreover, the osteoclast number was also significantly reduced in *OC-Cre;Men1$^{f/f}$* mice compared with control mice (Fig. 3*C*, *i* and *ii*). These findings suggest that osteoblast menin plays an important role in bone formation as well as bone turnover and is critical for maintenance of normal bone remodeling. In addition, osteocyte numbers were increased in *OC-Cre;Men1$^{f/f}$* mice relative to controls (Fig. 3*D*, *i* and *ii*).

Osteoblast-specific Deletion of the Men1 Gene Decreases Osteoclastogenesis—Multinucleated osteoclasts formed from the bone marrow of *OC-Cre;Men1$^{f/f}$* mice and cultured with exogenous M-CSF and RANKL were no different in appearance and number from those of *Men1$^{f/f}$* mice (Fig. 4*A*, *i* and *ii*). However, in co-culture experiments in which osteoclastogenesis relies on the endogenous factors produced by osteoblasts formed by treatment with ascorbic acid a clear difference was observed. First, osteoblast formation assessed by alkaline phosphatase staining was reduced in the marrow co-cultures of the *OC-Cre;Men1$^{f/f}$* mice relative to those of *Men1$^{f/f}$* mice (Fig. 4*B*, *i* and *ii*). Second, osteoclastogenesis was significantly reduced, as assessed by total TRAP-positive cells, in the menin osteoblast knock-out mice relative to that in control mice (Fig. 4*C*, *i* and *ii*). Finally, multinucleated osteoclasts quantified in fluorescently labeled cells were markedly deficient in the marrow co-cultures of the osteoblast menin knock-out mice *versus* those of the control mice (Fig. 4*D*, *i* and *ii*).

Hence, although the generation of osteoclasts from the bone marrow cells of the knock-out *OC-Cre;Men1$^{f/f}$* mice was unimpaired when exogenous M-CSF and RANKL were added, the bone marrow cells of the knock-out mice demonstrated markedly deficient osteoclastogenesis when only ascorbate was added to stimulate osteoblast differentiation without added osteoclastogenic factors.

Primary Cultures of Calvarial Osteoblasts of Neonatal and Adult Mice—Primary osteoblasts were isolated from individual calvaria of 2-week-old (neonatal) and 6-month-old (adult)

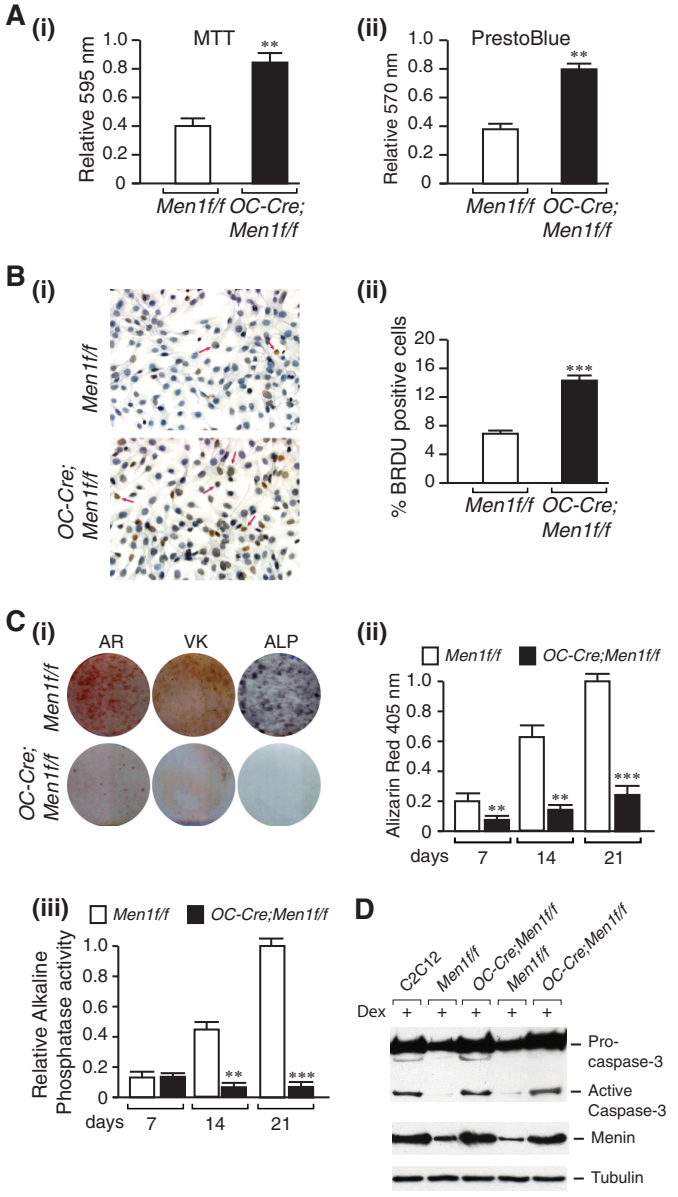

FIGURE 5. **Increased proliferation, impaired mineral apposition, and ALP activity and increased susceptibility to apoptosis of menin-deficient calvarial osteoblasts.** Primary osteoblasts were isolated from individual calvaria of 6-month-old *Men1*$^{f/f}$ (control) and *OC-Cre;Men1*$^{f/f}$ (osteoblast knock-out) mice and cultured for 7–10 days in αMEM, and the following assays were then carried out. *A*: *i*, MTT dye viability assay. Absorbance was read at 595 nm. Values shown are the mean ± S.E. ($n = 3$ independent experiments). **, $p < 0.01$. *ii*, PrestoBlue cell viability assay. Absorbance was read at 570 nm and normalized to the 600-nm value. Values shown are the mean ± S.E. ($n = 3$ independent experiments). **, $p < 0.01$. *B*, cell proliferation was assessed by BrdU incorporation. *i*, staining. *ii*, quantitation. ***, $p < 0.001$. *C*, Alizarin Red-S (*AR*) staining. Primary osteoblasts were plated in an osteogenic medium containing β-glycerophosphate and L-ascorbic acid. *i*, cells were fixed at 7, 14, and 21 days (shown) and stained with Alizarin Red-S. *ii*, quantitation was made by extraction and measurement of absorbance at 405 nm. Values are the mean ± S.E. ($n = 3$ independent experiments). **, $p < 0.01$. *C*: *i*, von Kossa (*VK*) staining. Primary osteoblasts were plated in an osteogenic medium. Phosphate deposition was evaluated at 14 and 21 days (shown) post-differentiation by staining fixed cells with von Kossa solution. Washed cells were scanned. *C*, ALP. Primary osteoblasts were cultured in an osteogenic medium for 7, 14, and 21 days (shown). *i*, ALP staining. Washed, fixed cells were overlaid with nitro blue tetrazolium chloride)/BCIP (5-bromo-4-chloro-3′-indolyl phosphate *p*-toluidine salt) (NBT) and incubated at room temperature for 20 min in the dark. *iii*, ALP activity. *p*-Nitrophenyl phosphate substrate was added to lysed cell extracts, and the reaction was stopped with 3 N NaOH. Absorbance was read at 405 nm, and values were normalized to protein concentration. Values are the mean ± S.E. ($n = 3$ independent experiments). **, $p < 0.01$; ***, $p < 0.001$. *D*, mouse C2C12 cells and adult primary osteoblasts originating from individual mice were seeded at a density of 1×10^6 in 60 mm plates. After 48 h cells were treated (+) or not with 1 mM dexamethasone (*Dex*) and incubated for a further 24 h. Proteins in cell lysates were separated by SDS-PAGE, transferred to PVDF membranes, and Western-blotted overnight at 4 °C with anti-caspase-3 antibody or anti-menin antibody followed by HRP-conjugated secondary antibody. Detection was performed using enhanced chemiluminescence. *First lane*, C2C12 cells; *second* and *fourth lanes*, *Men1*$^{f/f}$ osteoblasts; *third* and *fifth lanes*, *OC-Cre;Men1*$^{f/f}$ osteoblasts.

Men1$^{f/f}$ (control) and *OC-Cre;Men1*$^{f/f}$ (osteoblast knock-out) mice. Once established, the cells were replated and grown until confluent and RNA was isolated. By semiquantitative RT-PCR both the neonatal and adult *OC-Cre;Men1*$^{f/f}$ osteoblasts expressed markedly reduced levels of menin mRNA compared with the *Men1*$^{f/f}$ controls. Both the neonatal and adult *OC-Cre;Men1*$^{f/f}$ osteoblasts demonstrated similar alterations with respect to proliferation, mineral apposition, differentiation, and gene expression relative to the *Men1*$^{f/f}$ control osteoblasts. Therefore, detailed data are presented only for osteoblasts isolated from the adult mice.

Menin-deficient Calvarial Osteoblasts Exhibit Increased Proliferation and Impaired Mineral Apposition and ALP Activity—By MTT and PrestoBlue viability assays (Fig. 5*A*, *i* and *ii*) and BrdU assay (Fig. 5*B*, *i* and *ii*), primary calvarial osteoblasts of the adult *OC-Cre;Men1*$^{f/f}$ mice proliferated more rapidly than those of the *Men1*$^{f/f}$ controls. By Alizarin Red-S staining for calcium deposition (Fig. 5*C*, *i* and *ii*), von Kossa staining for phosphate deposition (Fig. 5*Ci*) primary calvarial osteoblasts of the adult *OC-Cre;Men1*$^{f/f}$ mice were markedly impaired with respect to mineral apposition relative to those of the *Men1*$^{f/f}$ control mice. Likewise, the primary calvarial osteoblasts of the adult *OC-Cre;Men1*$^{f/f}$ mice were markedly impaired with respect to ALP staining (Fig. 5*Ci*) and activity (Fig. 5*Ciii*) compared with those of the *Men1*$^{f/f}$ control mice.

Menin-deficient Osteoblasts Undergo Caspase-3 Cleavage More Readily Than Wild Type—To assess the ability of the menin-deficient osteoblasts to undergo apoptosis, we examined the extent of procaspase-3 cleavage promoted by dexamethasone. Control mouse C2C12 cells or *Men1*$^{f/f}$ or *OC-Cre;Men1*$^{f/f}$ calvarial osteoblasts were stimulated or not with 1 μM dexamethasone for 24 h. Cell extracts were subjected to SDS-PAGE and Western blot analysis with anti-caspase-3 antibody. Whereas the dexamethasone treatment clearly stimulated cleavage of pro-caspase-3 and production of the active caspase-3 17-kDa fragment in the control C2C12 and the *OC-Cre;Men1*$^{f/f}$, cells this was not apparent in the control osteoblasts (Fig. 5*D*). Hence, the menin-deficient osteoblasts are more susceptible to apoptotic stimuli than the control osteoblasts. This result is consistent with the TUNEL assay results on vertebral sections showing enhanced apoptotic rate of osteoblasts in the menin knock-out *versus* control mice (Fig. 3*B*, iii and *iv*).

Reduced TGF-β and BMP-2 Transcriptional Responsiveness in Menin-deficient Calvarial Osteoblasts—To assess their TGFβ ligand family transcriptional responsiveness, primary calvarial osteoblasts were transfected with promoter-reporter constructs, p3TP-Lux or Xvent-2, responsive to TGFβ or BMP-2, respectively. The *OC-Cre;Men1*$^{f/f}$ cells were impaired relative to the *Men1*$^{f/f}$ control cells with respect to ligand-stimulated luciferase

reporter activity;1.5-fold *versus* 3.5-fold basal, respectively, for both TGFβ and BMP-2 (Fig. 6*A*, *left* and *right panels*).

Altered Expression of Genes Involved in Osteoblast Differentiation and Proliferation, Osteoclast Formation, Osteocyte Formation, and Apoptosis—To examine the effect of osteoblast *Men1* loss on gene expression, semi-quantitative RT-PCR was performed on RNA from isolated osteoblasts from the *Men1* knock-out and control mice. The expression of key osteoblast marker genes for BMP-2, Runx2, Osterix, Dlx5, Col1a1 and osteocalcin, were reduced in osteoblasts from adult OC-Cre; $Men1^{f/f}$ mice relative to those from control mice (Fig. 6*B*). These genes are all under the control, either directly or indi-

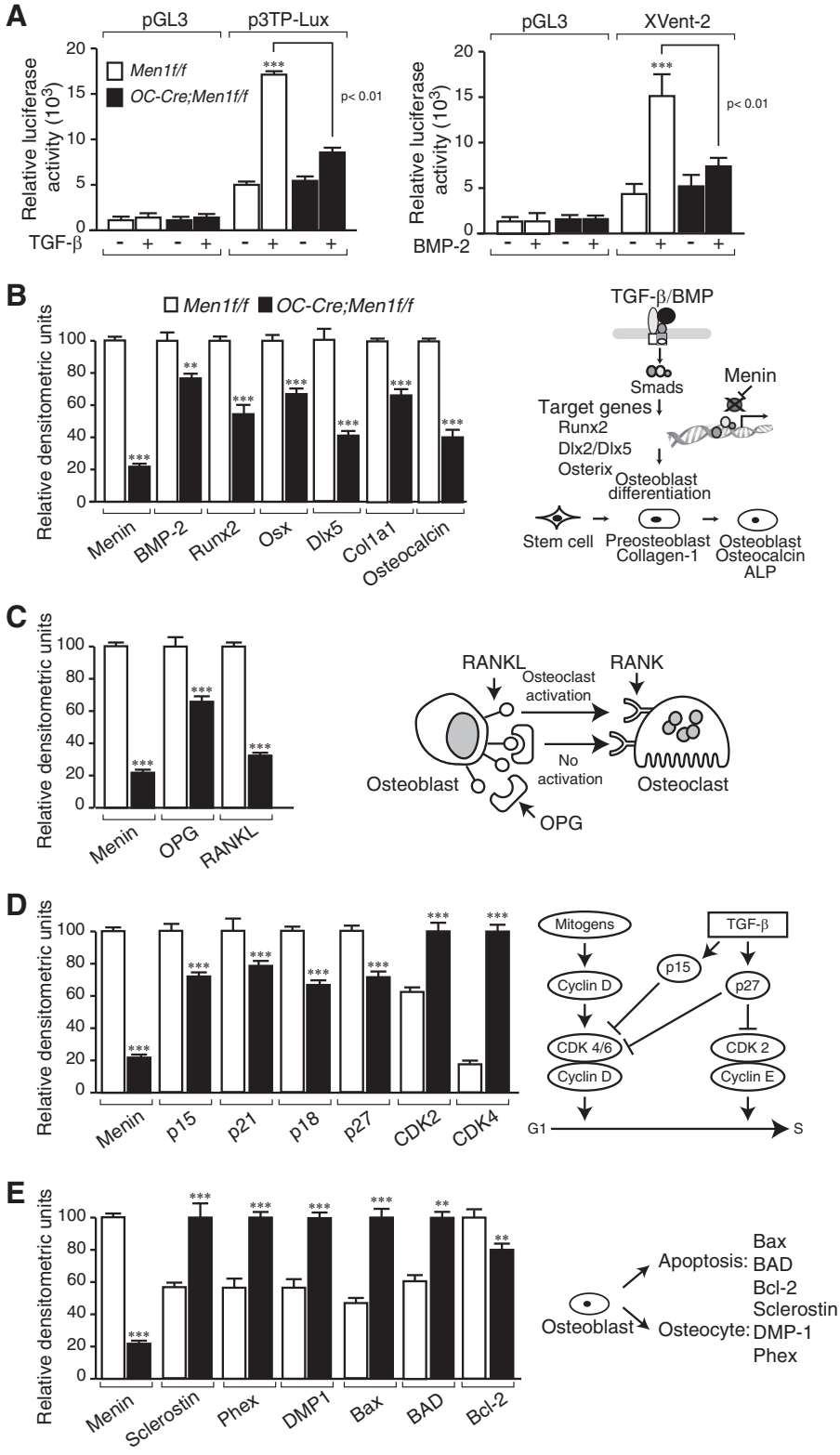

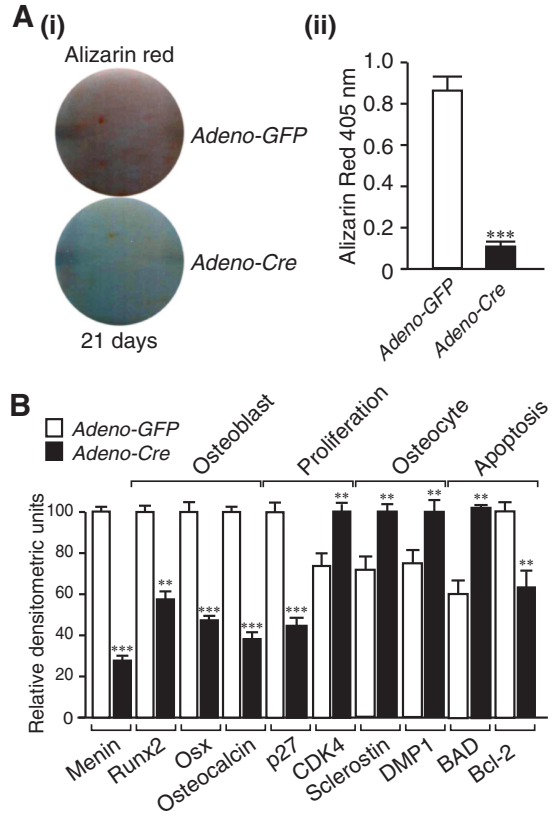

FIGURE 7. **Reduced mineralization and altered gene expression by direct deletion of menin in osteoblasts.** Primary calvarial *Men1*$^{f/f}$ osteoblasts were infected with adenovirus expressing GFP (control) or Cre recombinase. *A*, mineralization was assessed by Alizarin Red-S assay. *i*, staining at 21 days after culture in osteogenic medium. *ii*, quantitation. ***, $p < 0.001$; Adeno-Cre *versus* Adeno-GFP. *B*, RNA was isolated, semiquantitative RT-PCR and gel electrophoresis was performed, and densitometric analysis was made. Expression of osteoblast markers Runx2, Osx, and osteocalcin was reduced, the cyclin-dependent kinase inhibitor p27 was reduced, CDK4 was increased, osteocyte markers sclerostin and DMP-1 were increased, pro-apoptotic marker Bad was increased, and anti-apoptotic marker Bcl-2 was decreased. **, $p < 0.01$; ***, $p < 0.001$; *Adeno-Cre versus Adeno-GFP*.

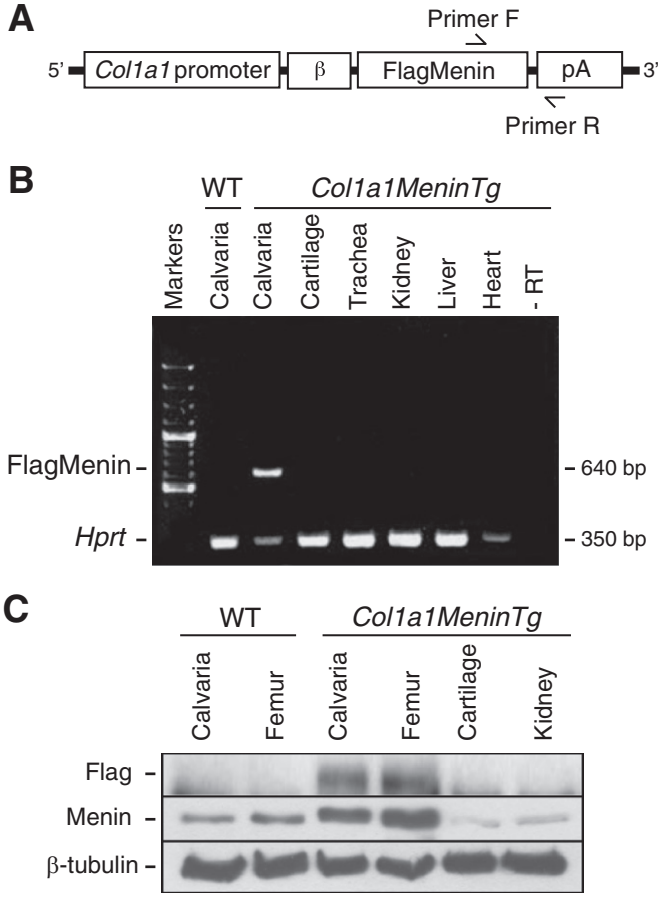

FIGURE 8. **Osteoblast-specific overexpression of menin.** *A*, *Col1a1-Menin-Tg* transgene construct in which the osteoblast-specific 2.3-kb *Col1a1* promoter drives expression of a FLAG-tagged human menin cDNA. β, rabbit β-globin intron; *pA*, SV40 polyadenylation signal. *Arrows* indicate positions of forward (*F*) and reverse (*R*) primers. *B*, tissue RNA (calvaria, cartilage, trachea, kidney, liver, and heart) was extracted, and RT-PCR was carried out. The *Col1a1-Menin-Tg* transgene was expressed specifically in bone in the founder shown. −*RT*, minus reverse transcriptase control. *C*, tissue protein (calvaria, femur, cartilage, and kidney) was extracted, and a Western blot was conducted with antibodies against FLAG (*Col1a1-Menin-Tg* transgene), menin (endogenous and exogenous menin), and β-tubulin (loading control). The transgene (menin) was expressed specifically in bone of the *Col1a1-Menin-Tg* mice.

rectly, of the BMP/TGF-β signaling pathways. Although the expression of both OPG and RANKL was decreased in osteoblasts from adult *OC-Cre;Men1*$^{f/f}$ mice relative to controls, the relative decrease for RANKL was greater, favoring an increase in the OPG/RANKL ratio (Fig. 6*C*). This would be consistent with the finding of reduced numbers of osteoclasts in the *OC-Cre;Men1*$^{f/f}$ mice (Fig. 3*C*, *i* and *ii*) as well as the impaired support of osteoclastogenesis observed in the co-culture assays with bone marrow of the osteoblast menin knock-out *versus* control mice (Fig. 4, *A*–*D*). Expression of TGF-β target genes important for cell cycle and/or differentiation control was also altered, being either down-regulated (p15, p21, p18, p27) or up-regulated (CDK2 and CDK4) in *OC-Cre;Men1*$^{f/f}$ osteoblasts (Fig. 6*D*). These results are consistent with the finding that osteoblasts from *OC-Cre;Men1*$^{f/f}$ mice proliferated more rapidly relative to controls (Figs. 5*B*, *i* and *ii*). Expression of osteocyte markers, Sclerostin, Phex, and DMP-1, was higher in osteoblasts from *OC-Cre;Men1*$^{f/f}$ mice relative to controls (Fig. 6*E*). Expression of proapoptotic markers Bax and Bad was

FIGURE 6. **Reduced TGF-β- and BMP-2-transcriptional responsiveness in menin-deficient calvarial osteoblasts.** Primary osteoblasts were isolated from individual calvaria of 6-month-old *Men1*$^{f/f}$ (control) and *OC-Cre;Men1*$^{f/f}$ (osteoblast knock-out) mice and cultured for 7–10 days in αMEM. Cells were plated at a density of 1×10^5 cells per 35-mm dish and grown until confluent (2–3 days). *A*: *left panel*, the promoterless pGL3 or the TGF-β-responsive 3TP-Lux promoter-reporter constructs were transfected into the osteoblasts that were then stimulated (+) or not (−) with TGF-β. Relative luciferase activity was measured, and the values shown represent the mean ± S.E. ***, $p < 0.001$. TGF-β (+) *versus* (−). *Right panel*, the promoterless pGL3 or the BMP-2-responsive Xvent2 promoter-reporter constructs were transfected into the osteoblasts that were then stimulated (+) or not (−) with BMP-2. Relative luciferase activity was measured, and the values shown represent the mean ± S.E. ***, $p < 0.001$. BMP-2 (+) *versus* (−). Gene expression changes in calvarial osteoblasts of *OC-Cre;Men1*$^{f/f}$ mice is shown. Osteoblasts were isolated and cultured as described above. *B*–*E*, RNA was isolated, semiquantitative RT-PCR and gel electrophoresis were performed, and densitometric analysis was made. *B*, expression of osteoblast markers, BMP-2, Runx2, Osx, Dlx5, Col1a1, and Osteocalcin, was reduced in the *OC-Cre;Men1*$^{f/f}$ osteoblasts. *C*, expression of both OPG and RANKL was reduced in the *OC-Cre;Men1*$^{f/f}$ mice, with the relative decrease for RANKL being greater. *D*, expression of the CDKIs, p15, p21, p18, and p27 was reduced, whereas that of CDK2 and CDK4 was increased in the *OC-Cre;Men1*$^{f/f}$ osteoblasts. *E*, expression of the osteocyte markers, Sclerostin, Phex, and DMP-1, was increased in the *OC-Cre;Men1*$^{f/f}$ mice. Expression of the pro-apoptotic markers Bax and Bad were increased and that of the anti-apoptotic marker Bcl-2 was decreased. **, $p < 0.01$; ***, $p < 0.001$; *OC-Cre;Men1*$^{f/f}$ *versus Men1*$^{f/f}$.

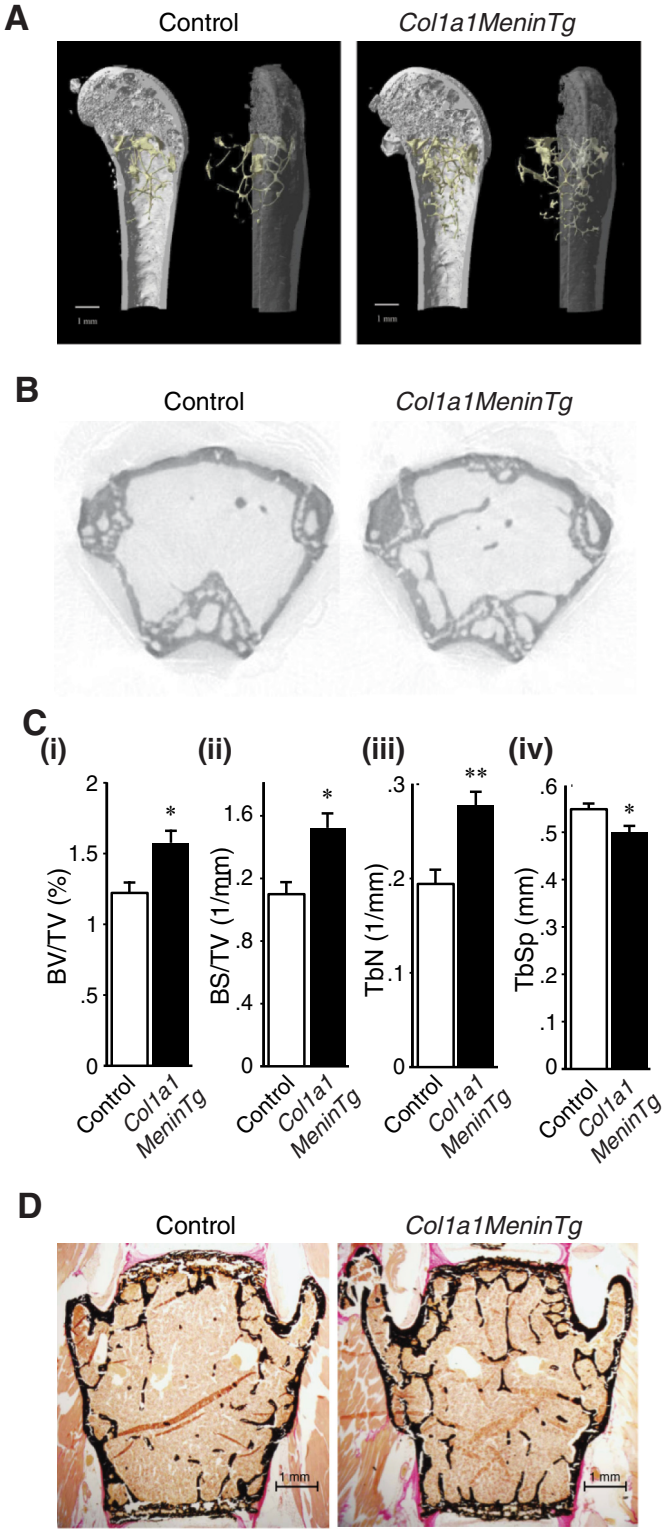

FIGURE 9. **Overexpression of osteoblast menin enhances bone parameters.** *A*, representative images of micro-CT analysis of distal femur of 12-month-old *Col1a1-Menin-Tg* ($n = 4$) and control mice ($n = 5$). *B*, trabecular bone was increased in *Col1a1-Menin-Tg* mice compared with controls. *C*, *bar graphs* show BV/TV (*i*), BS/TV (*ii*), and trabecular number (*TbN*) (*iii*), of *Col1a1MeninTg* mice ($n = 4$) were significantly higher, whereas (*iv*) trabecular separation (*TbSp*) was significantly lower than those of controls ($n = 4$). *, $p < 0.05$; **, $p < 0.01$. See Table 2. Overexpression of osteoblast menin increased trabecular bone assessed by histomorphometry. *D*, representative images of von Kossa/van Gieson staining of vertebrae of 12-month-old *Col1a1-Menin-Tg* and control mice. See Table 2.

TABLE 2

BMD, three-dimensional micro-CT and histological analysis of femur, and histomorphometric analysis of lumbar spine from 12-month-old female Col1a1-Menin-Tg and control mice

Tb, trabecular number; TbSp, trabecular separation; SMI, structure model index; TbTh, trabecular thickness; TbN, trabecular number; CtTh, cortical bone thickness; NS, not significant.

Parameter	Control	*Col1a1-Menin-Tg*	Significance
BMD (g/cm^2)	0.067 ± 0.0007	0.07 ± 0.009	NS
Micro-CT			
BV/TV (%)	0.93 ± 0.17	1.57 ± 0.09	$p < 0.05$
BS/BV (mm^2/mm^3)	99.26 ± 7.52	96.36 ± 3.74	NS
BS/TV (mm^2/mm^3)	0.89 ± 0.12	1.51 ± 0.09	$p < 0.01$
SMI	2.88 ± 0.08	2.63 ± 0.03	$p < 0.05$
TbTh (mm)	0.06 ± 0.004	0.06 ± 0.0006	NS
TbN (1/mm)	0.15 ± 0.03	0.28 ± 0.01	$p < 0.05$
TbSp (mm)	0.56 ± 0.01	0.50 ± 0.02	NS
CtTh (mm)	0.20 ± 0.01	0.19 ± 0.01	NS
Histomorphometry			
BV/TV (%)	5.67 ± 0.41	7.51 ± 0.66	$p < 0.05$
BS/TV (mm^2/mm^3)	4.32 ± 0.49	5.76 ± 0.47	$p < 0.05$
BS/BV (mm^2/mm^3)	75.41 ± 3.96	77.32 ± 3.05	NS
TbTh (μm)	26.80 ± 1.32	26.04 ± 1.09	NS

higher, whereas that of the anti-apoptotic Bcl-2 was lower (Fig. 6*E*). Taken together with the *in vivo* findings, the osteoblast gene expression data would suggest that the menin-deficient osteoblasts are functionally defective but proliferate more rapidly to the point at which they become osteocytes or undergo apoptosis. The reprogramming of the osteoblast gene expression profile occurs early as identical changes to those in the adult osteoblasts were found in neonatal osteoblasts of the *OC-Cre;Men1$^{f/f}$* mice relative to controls (data not shown).

Disruption of Men1 in Primary Calvarial Osteoblasts in Vitro—To assess the effect of directly disrupting the osteoblast *Men1* gene *in vitro*, primary adult *Men1$^{f/f}$* osteoblasts were infected with either Adeno-Cre or Adeno-GFP. The Adeno-Cre-infected cells in which menin expression was reduced by >70% relative to the Adeno-GFP-infected controls demonstrated markedly reduced mineralization by Alizarin Red-S assay (Fig. 7*A*, *i* and *ii*). Gene expression analysis by semiquantitative RT-PCR indicated decreases in osteoblast markers, increases in osteocyte markers, and altered proliferation and apoptotic genes (Fig. 7*B*). These changes were all similar to the findings in primary calvarial osteoblasts of the *OC-Cre;Men1$^{f/f}$* mice relative to controls (Figs. 5*C* and 6, *B–E*).

Specific Osteoblast Overexpression of Menin Increases Bone Mass Accumulation—To overexpress *Men1* specifically in osteoblasts *in vivo*, we made a *Col1a1-Menin* transgene construct in which a 2.3-kb *Col1a1* promoter fragment drives a human FLAG-tagged menin cDNA (Fig. 8*A*). Pronuclear injection of the construct into fertilized mouse eggs resulted in seven founders of which two demonstrated bone-specific expression of menin. The mice were then mated with wild-type mice. *Col1a1-Menin-Tg* mice generated from this breeding were analyzed for transgene expression using semiquantitative reverse transcriptase PCR, showing that the transgene was expressed only in bone tissue (Fig. 8*B*). The overexpression of menin in bone was confirmed by Western blot analysis (Fig. 8*C*).

Col1a1-Menin-Tg mice were no different from controls with respect to weight (g) (35.0 ± 1.0 *versus* 35.0 ± 1.5) and in serum levels (mmol/liter) of calcium (2.6 ± 0.1 *versus* 2.4 ± 0.2), phosphate (2.6 ± 0.2 *versus* 2.2 ± 0.2), and magnesium (1.3 ± 0.1

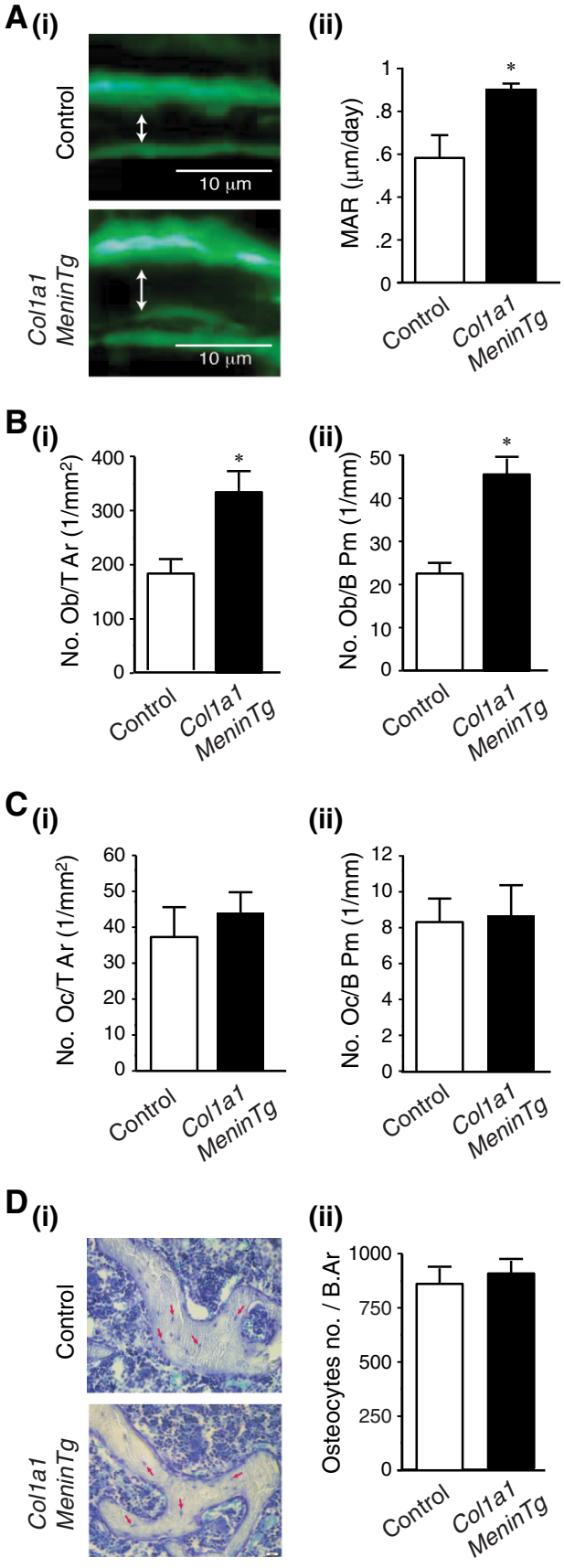

FIGURE 10. **Overexpression of menin in osteoblasts increases osteoblast number and bone formation.** *A*, Twelve-month-old female mice were labeled with sequential doses of calcein, and dynamic indices of bone formation were quantitated in *Col1a1-Menin-Tg* ($n = 3$) and control mice ($n = 3$). *i*, representative section. *ii*, MAR was significantly increased in *Col1a1-Menin-Tg* mice relative to controls. *, $p < 0.05$. *B*, *i* and *ii*, numbers of osteoblasts are significantly increased in the *Col1a1-Menin-Tg* mice ($n = 3$) *versus* controls ($n = 3$). *, $p < 0.05$. *C*, *, $p < 0.05$. *C*, *i* and *ii*, numbers of osteoclasts are no different in the *Col1a1-Menin-Tg* mice ($n = 3$) *versus* controls ($n = 3$). *Oc/T Ar*, osteoclast tissue area; *Oc/B Pm*, osteoclast bone perimeter. *D*, *i* and *ii*, numbers of osteocytes are no different in the *Col1a1-Menin-Tg* mice ($n = 3$) *versus* controls ($n = 3$).

versus 1.3 ± 0.1) at 12 months of age. Although there was no significant difference in BMD (g/cm2) at the femurs (0.07 ± 0.001 *versus* 0.068 ± 0.004) of *Col1a1-Menin-Tg* mice compared with wild-type littermates, micro-CT analysis showed increases in trabecular bone (Fig. 9, *A* and *B*). There were significant increases in bone volume and surface and trabecular numbers as well as decreases in structure model index and trabecular spacing (Fig. 9*C*, *i–iv*; Table 2). Furthermore, von Kossa/van Gieson staining of lumbar vertebrae indicated that trabecular bone was increased in *Col1a1-Menin-Tg* mice compared with controls (Fig. 9*D*). By histomorphometric analysis, bone volume and surface were significantly increased in *Col1a1-Menin-Tg* mice (Fig. 9*D*; Table 2). Cancellous MAR was significantly increased in *Col1a1-Menin-Tg* mice compared with control mice (Fig. 10*A*, *i* and *ii*), and the number of osteoblasts was significantly increased in *Col1a1-Menin-Tg* mice (Fig. 10*B*, *i* and *ii*), although the numbers of osteoclasts (Fig. 10*C*, *i* and *ii*) and osteocytes were not altered (Fig. 10*D*, *i* and *ii*). Therefore, to a large extent the bone phenotype of the *Col1a1-Menin-Tg* mirrors that of the *OC-Cre;Men1$^{f/f}$* mice.

Effect of Menin Overexpression in the Osteoblast on Proliferation, Differentiation, Mineralization, and Gene Expression—Primary calvarial osteoblasts were isolated from adult *Col1a1-Menin-Tg* mice. The *Col1a1-Menin-Tg* osteoblasts demonstrated reduced numbers in cell viability MTT and Prestoblue assays (Fig. 11*A*, *i* and *ii*), increased mineralization by Alizarin Red-S assay (Fig. 11*B*, *i* and *ii*), and increased alkaline phosphatase differentiation marker activity (Fig. 11*C*, *i* and *ii*). Therefore, the phenotype of the *Col1a1-Menin-Tg* primary calvarial osteoblasts largely mirrors that of the *OC-Cre;Men1$^{f/f}$* mice osteoblasts. By semiquantitative RT-PCR, osteoblast differentiation markers, Runx2, osteocalcin, and Col1a1, were increased, as were CDKIs, p15, and p21, whereas CDK4 was decreased (Fig. 11*D*). These changes mirrored those in the *OC-Cre;Men1$^{f/f}$* mice osteoblasts. Expression of RANKL, OPG, and Sclerostin as well as Bax and Bcl-2 were unchanged in the *Col1a1-Menin-Tg* primary osteoblasts relative to controls (Fig. 11*D*). These data are consistent with the unchanged osteoclast and osteocyte numbers and suggest that susceptibility to apoptosis is unaltered. The fact that overexpressing menin did not affect osteoclast-modulating, osteocytic, and apoptosis-related genes whereas deleting menin increased these genes suggests that there is a threshold at which the level of menin is sufficient for an effect on a particular gene. Therefore, the data suggest that the thresholds are different for different genes (and importantly for different subsets of genes).

DISCUSSION

We investigated the role of menin in bone by using a Cre-mediated recombination strategy to conditionally disrupt the *Men1*

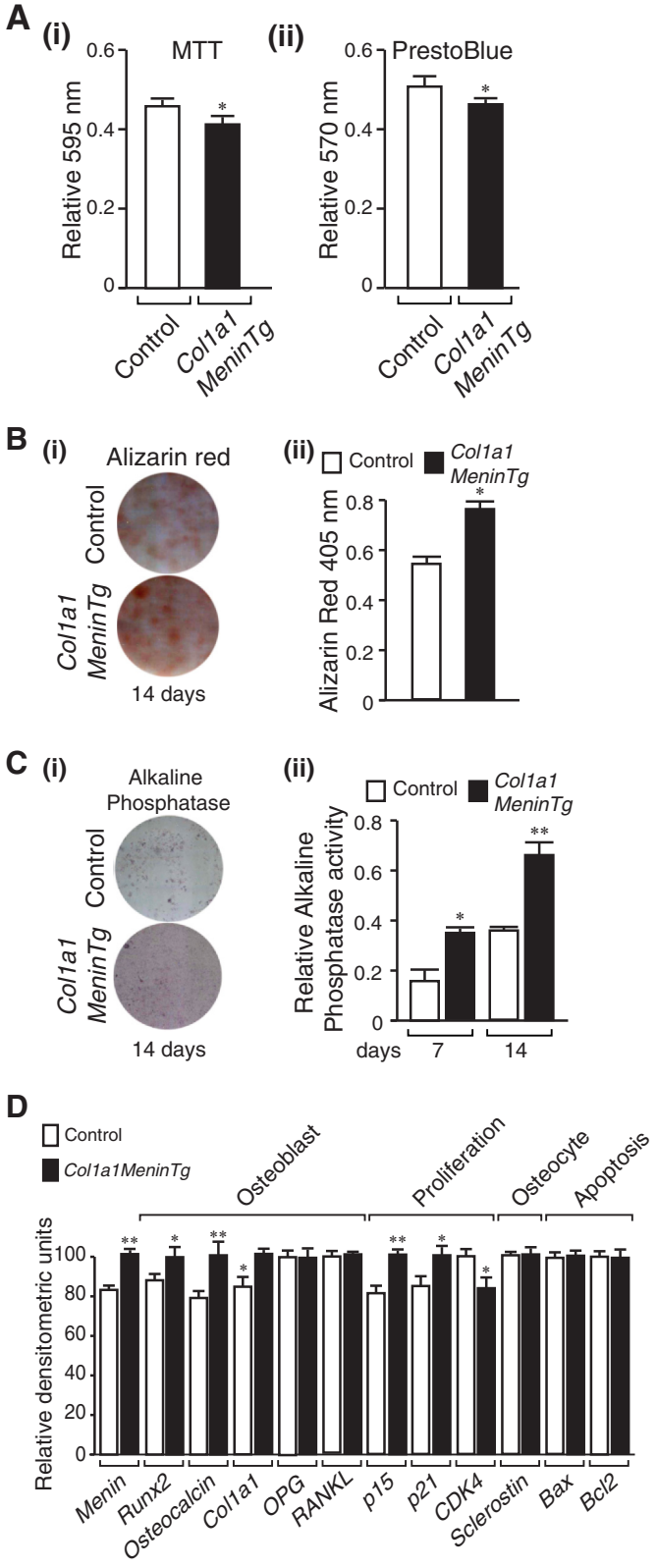

FIGURE 11. **Decreased proliferation, increased mineral apposition, and ALP activity and altered gene expression of menin-deficient calvarial osteoblasts.** Primary osteoblasts were isolated from individual calvaria of 12-month-old *Col1a1-Menin-Tg* and control mice and cultured for 7–10 days in αMEM, and the following assays were then carried out. *A*: *i*, MTT dye viability assay. Absorbance was read at 595 nm. Values shown are mean ± S.E. ($n = 3$ independent experiments). *, $p < 0.05$. (ii) PrestoBlue cell viability assay. Absorbance was read at 570 nm and normalized to the 600-nm value. Values shown are the mean ± S.E. ($n = 3$ independent experiments). *, $p < 0.05$. *B*, Alizarin Red-S staining. Primary osteoblasts were plated in an osteogenic medium. *i*, cells were fixed at 14 days and stained with Alizarin Red-S. *ii*, quantitation was made by extraction and measurement of absorbance at 405 nm. Values are the mean ± S.E. ($n = 3$ independent experiments). *, $p < 0.05$. *C*, ALP. Primary osteoblasts were cultured in an osteogenic medium containing β-glycerophosphate and L-ascorbic acid for 7 and 14 days (shown). *i*, ALP staining. Washed, fixed cells were overlaid with nitro blue tetrazolium chloride)/BCIP (5-bromo-4-chloro-3′-indolyl phosphate p-toluidine salt) (NBT) and incubated at room temperature for 20 min in the dark. *ii*, ALP activity. *p*-Nitrophenyl phosphate substrate was added to lysed cell extracts, and the reaction was stopped with 3 N NaOH. Absorbance was read at 405 nm, and values were normalized to protein concentration. Values are the mean ± S.E. ($n = 3$ independent experiments). *, $p < 0.05$; **, $p < 0.01$. *D*, RNA was isolated, semi-quantitative RT-PCR and gel electrophoresis were performed, and densitometric analysis was made. Expression of osteoblast markers Runx2, osteocalcin, and Col1a1 was increased, OPG and RANKL were unaltered, the CDKIs p15 and p21 were increased, CDK4 was decreased, and the osteocyte marker Sclerostin, the pro-apoptotic Bax, and the pro-survival Bcl-2 were unaltered. *, $p < 0.05$; **, $p < 0.01$ *Col1a1-Menin-Tg versus* control.

gene in osteoblasts as well as overexpressing menin specifically in osteoblasts. We show that menin is important for proper osteoblast function and maintenance of bone mass *in vivo*.

The tumor suppressor menin is encoded by the *MEN1* gene in which germ line mutations cause the autosomal dominant MEN1 disorder characterized by the development of tumors in select endocrine (and non-endocrine) tissues (6, 7). Menin is widely expressed from early in fetal development. Heterozygous constitutional knock-out *Men1*$^{+/-}$ mice closely mimic their human MEN1 counterparts and from 9 months of age develop hyperplasia and tumors of parathyroid and anterior pituitary glands and pancreatic islets (10–12). Mice having tissue-specific knock-out of the *Men1* gene in parathyroid, pituitary, or pancreatic β-cells develop normally, suggesting that menin does not influence development of these tissues (13–16). However, constitutively null *Men1*$^{-/-}$ mice die *in utero* at midgestation of multiple defects in developing organs, suggesting that menin is critical for normal development (10, 17, 18). The fetuses are small and have craniofacial defects suggesting that menin might play a role in both endochondral and intramembranous bone formation (10, 17). We showed previously that menin promotes the commitment of mesenchymal stem cells *in vitro* to the osteoblast lineage (19). This occurs in part by the roles played by menin in facilitating BMP-2 signaling via Smads and transcriptional activity of the key osteoblast regulator, Runx2 (20). Menin interacts physically and functionally with Smads1/5 and Runx2 in mesenchymal stem cells. In committed osteoblasts, menin appears to restrain the osteoblasts in their differentiated state, and this is achieved in part by menin's interaction with the TGF-β/Smad3 pathway (20).

In mesenchymal stem cells *in vitro* inactivation of menin only affects the BMP-2-induction of osteoblasts and apparently has little effect on generation of chondrocytes or adipocytes (19). In addition, others have shown that by modulating responsiveness to the cytokines TGF-β and BMP-2, menin functions to shift the balance of multipotential mesenchymal cell commitment to the osteogenic rather than the myogenic lineage (36). *In vivo* deletion of the *Men1* gene in Pax3- or Wnt1-expressing neural crest cells (that give rise to many cell lineages including the mesenchymal stem cells that become osteoblasts) leads to perinatal death, cleft palate, and other cranial bone defects (37).

Deletion of menin in Pax3-expressing somite precursors also produces patterning defects of rib formation (37).

In the present studies we have taken the direct approach of deleting the *Men1* gene, on the one hand, and of overexpressing menin, on the other, in the osteoblast. This has provided validation that menin is important *in vivo* for osteoblast function and maintenance of bone mass. The *Men1* osteoblast knock-out mice displayed significant reduction in bone mineral density, trabecular bone volume, and cortical bone thickness compared with their control littermates. Osteoblast and osteoclast numbers as well as mineral apposition rate were significantly reduced, whereas osteocyte number was increased. Primary calvarial osteoblasts proliferated more quickly but exhibited deficient mineral apposition and reduced alkaline phosphatase activity. In contrast to the knock-out mice, transgenic mice overexpressing osteoblast menin showed a gain of bone mass, and osteoblast number and mineral apposition rate were increased relative to their control littermates.

The gene expression analysis of osteoblasts *in vitro* provided insights into alterations that underlie the *in vivo* phenotype of the *Men1* knock-out mice. Promoter-reporter assays demonstrated that the menin-deficient osteoblasts were impaired with respect to their ability to respond normally at the transcriptional level to either TGF-β or BMP-2. This was consistent with the finding of reduced expression of key osteoblast markers such as BMP-2 itself and Runx2, Osterix, Dlx2, Dlx5, and osteocalcin. These genes are all under the control, either directly or indirectly, of the BMP-2/TGF-β signaling pathways. As a consequence, *in vivo* osteoblast number, bone formation, and bone mass were reduced.

Production of the bone resorbing cell, the osteoclast, is stimulated by the RANKL synthesized by the osteoblast that acts via cell-cell contact on RANK expressed by the osteoclast precursor (38). The relative expression of the decoy receptor, OPG, secreted by the osteoblast, is also key in dictating the final outcome with respect to osteoclast generation (39). Although the expression of both OPG and RANKL, was decreased in menin-deficient osteoblasts, that of RANKL was greater, favoring an increase in the OPG/RANKL ratio. This would be consistent with the finding of reduced numbers of osteoclasts in the osteoblast *Men1* knock-out mice and their decreased ability to support osteoclastogenesis in the bone marrow co-culture assays. As bone formation and bone resorption are coupled (40), the findings identify impaired bone remodeling as an additional underlying cause of the reduced bone volume in the Men1 osteoblast knock-out mice.

Expression of genes important for cell cycle control was also altered, with that for CDKIs, p15, p18, p21, p27, being down regulated, whereas that for CDK2 and CDK4 being up-regulated. This was all consistent with the proliferation rate of the menin-deficient osteoblasts being greater than those of the controls. Osteocyte markers (Phex, DMP-1, and Sclerostin) were increased, and pro-apoptosis markers (Bax and Bad) were also increased, whereas that of the anti-apoptotic marker, Bcl-2, was decreased. These findings are consistent with the finding of increased numbers of osteocytes in the *Cre-OC;Men1$^{f/f}$* mice, on the one hand, and the enhanced apoptotic rate of osteoblasts observed *in vivo* as well as the enhanced susceptibility of primary calvarial *Cre-OC;Men1$^{f/f}$* osteoblasts *in vitro* to undergo apoptosis as indicated by a caspase-3 cleavage assay on the other hand. Given the fact that menin is required for the ability of BMPs to exert their effects on osteoblast differentiation via a Smad-dependent pathway (19, 20), it might be unexpected that menin-deficient osteoblasts exhibit more (rather than less) apoptosis. However, the present data are fully consistent with previous findings that BMP-2 promotes osteoblast apoptosis through a Smad-independent pathway (41).

Taken together with the *in vivo* findings, the gene expression data support the notion that the functionally defective osteoblasts proliferate to reach the point at which they either undergo apoptosis or become osteocytes much more quickly than normal. Hence, *in vivo*, osteoblast and osteocyte numbers are reduced and increased, respectively. Therefore, a lack of menin leads to a marked reprogramming of the osteoblast gene expression profile with subsequent phenotypic changes.

In summary, *Men1* osteoblast knock-out mice displayed a significant reduction of bone mass with decreases in osteoblast number, bone formation rate, and bone remodeling. On the other hand, bone volume was increased and bone formation was stimulated in transgenic mice overexpressing menin in the osteoblast. These findings suggest that menin is required for optimal bone formation and maintenance of bone mass. Primary osteoblasts from the *Men1* knock-out and the menin-overexpressing mice had altered gene expression profiles with respect to signaling pathways under the control of BMPs and TGF-β. In conclusion, menin, or more specifically the menin/Smad interface, can be considered as a potential gain of function therapeutic target for treatment of low bone mass disorders. The desired compounds would be those that mimic the effect of menin (as a transcriptional facilitator) upon the BMP receptor-regulated Smads.

Acknowledgments—We thank Xiang Zhou, Daouda Togola, and Geetanjali Nayak for technical support and Dr. Yongjun Xiao of the McGill Centre for Bone and Periodontal Research Core Facility, Dr. Ken Y.O. Cho for the Xvent2 construct, Dr. David Goltzman for technical advice, and Dr. David E.C. Cole for critical review of the manuscript.

REFERENCES

1. Chen, D., Zhao, M., Harris, S. E., and Mi, Z. (2004) Signal transduction and biological functions of bone morphogenetic proteins. *Front. Biosci.* **9,** 349–358
2. Otto, W. R., and Rao, J. (2004) Tomorrow's skeleton staff: mesenchymal stem cells and the repair of bone and cartilage. *Cell Prolif.* **37,** 97–110
3. Chen, G., Deng, C., and Li, Y.-P. (2012) TGF-β and BMP signaling in osteoblast differentiation and bone formation. *Int. J. Biol. Sci.* **8,** 272–288
4. Shi, Y., and Massagué, J. (2003) Mechanisms of TGF-β signaling from cell membrane to the nucleus. *Cell* **113,** 685–700
5. ten Dijke, P., Miyazono, K., and Heldin, C. H. (2000) Signaling inputs converge on nuclear effectors in TGF-β signaling. *Trends Biochem. Sci.* **25,** 64–70
6. Chandrasekharappa, S. C., Guru, S. C., Manickam, P., Olufemi, S. E., Collins, F. S., Emmert-Buck, M. R., Debelenko, L. V., Zhuang, Z., Lubensky, I. A., Liotta, L. A., Crabtree, J. S., Wang, Y., Roe, B. A., Weisemann, J., Boguski, M. S., Agarwal, S. K., Kester, M. B., Kim, Y. S., Heppner, C., Dong, Q., Spiegel, A. M., Burns, A. L., and Marx, S. J. (1997) Positional cloning of the gene for multiple endocrine neoplasia type 1. *Science* **276,** 404–407
7. Lemmens, I., Van de Ven, W. J., Kas, K., Zhang, C. X., Giraud, S., Wautot,

V., Buisson, N., De Witte, K., Salandre, J., Lenoir, G., Pugeat, M., Calender, A., Parente, F., Quincey, D., Gaudray, P., De Wit, M. J., Lips, C. J., Höppener, J. W., Khodaei, S., Grant, A. L., Weber, G., Kytölä, S., Teh, B. T., Farnebo, F., and Thakker, R. V. (1997) Identification of the multiple endocrine neoplasia type 1 (MEN1) gene. *Hum. Mol. Genet.* **6,** 1177–1183

8. Guru, S. C., Goldsmith, P. K., Burns, A. L., Marx, S. J., Spiegel, A. M., Collins, F. S., and Chandrasekharappa, S. C. (1998) Menin, the product of the MEN1 gene, is a nuclear protein. *Proc. Natl. Acad. Sci. U.S.A.* **95,** 1630–1634
9. Kaji, H., Canaff, L., Goltzman, D., and Hendy, G. N. (1999) Cell cycle regulation of menin expression. *Cancer Res.* **59,** 5097–5101
10. Crabtree, J. S., Scacheri, P. C., Ward, J. M., Garrett-Beal, L., Emmert-Buck, M. R., Edgemon, K. A., Lorang, D., Libutti, S. K., Chandrasekharappa, S. C., Marx, S. J., Spiegel, A. M., and Collins, F. S. (2001) A mouse model of multiple endocrine neoplasia type 1 develops multiple endocrine tumors. *Proc. Natl. Acad. Sci. U.S.A.* **98,** 1118–1123
11. Bertolino, P., Tong, W. M., Galendo, D., Wang, Z. Q., and Zhang, C. X. (2003) Heterozygous Men1 mutant mice develop a range of endocrine tumors mimicking multiple endocrine neoplasia type 1. *Mol. Endocrinol.* **17,** 1880–1892
12. Harding, B., Lemos, M. C., Reed, A. A., Walls, G. V., Jeyabalan, J., Bowl, M. R., Tateossian, H., Sullivan, N., Hough, T., Fraser, W. D., Ansorge, O., Cheeseman, M. T., and Thakker, R. V. (2009) Multiple endocrine neoplasia type 1 knockout mice develop parathyroid, pancreatic, pituitary, and adrenal tumours with hypercalcemia, hypophosphataemia and hypercorticosteronaemia. *Endocr. Relat. Cancer* **16,** 1313–1327
13. Libutti, S. K., Crabtree, J. S., Lorang, D., Burns, A. L., Mazzanti, C., Hewitt, S. M., O'Connor, S., Ward, J. M., Emmert-Buck, M. R., Remaley, A., Miller, M., Turner, E., Alexander, H. R., Arnold, A., Marx, S. J., Collins, F. S., and Spiegel, A. M. (2003) Parathyroid gland-specific deletion of the mouse *Men1* gene results in parathyroid neoplasia and hypercalcemic hyperparathyroidism. *Cancer Res.* **63,** 8022–8028
14. Crabtree, J. S., Scacheri, P. C., Ward, J. M., McNally, S. R., Swain, G. P., Montagna, C., Hager, J. H., Hanahan, D., Edlund, H., Magnuson, M. A., Garrett-Beal, L., Burns, A. L., Ried, T., Chandrasekharappa, S. C., Marx, S. J., Spiegel, A. M., and Collins, F. S. (2003) Of mice and MEN1: insulinomas in a conditional mouse knockout. *Mol. Cell. Biol.* **23,** 6075–6085
15. Biondi, C. A., Gartside, M. G., Waring, P., Loffler, K. A., Stark, M. S., Magnuson, M. A., Kay, G. F., and Hayward, N. K. (2004) Conditional inactivation of the Men1 gene leads to pancreatic and pituitary tumorigenesis but does not affect normal development of these tissues. *Mol. Cell. Biol.* **24,** 3125–3131
16. Bertolino, P., Tong, W.-M., Herrera, P. L., Casse, H., Zhang, C. X., and Wang, Z.-Q., (2003) Pancreatic β-cell-specific ablation of the multiple endocrine neoplasia type 1 (MEN1) gene causes full penetrance of insulinoma development in mice. *Cancer Res.* **63,** 4836–4841
17. Bertolino, P., Radovanovic, I., Casse, H., Aguzzi, A., Wang, Z. Q., and Zhang, C. X. (2003) Genetic ablation of the tumor suppressor menin causes lethality at mid-gestation with defects in multiple organs. *Mech. Dev.* **120,** 549–560
18. Lemos, M. C., Harding, B., Reed, A. A., Jeyabalan, J., Walls, G. V., Bowl, M. R., Sharpe, J., Wedden, S., Moss, J. E., Ross, A., Davidson, D., and Thakker, R. V. (2009) Genetic background influences embryonic lethality and the occurrence of neural tube defects in *Men1* null mice: relevance to genetic modifiers. *J. Endocrinol.* **203,** 133–142
19. Sowa, H., Kaji, H., Canaff, L., Hendy, G. N., Tsukamoto, T., Yamaguchi, T., Miyazono, K., Sugimoto, T., and Chihara, K. (2003) Inactivation of menin, the product of the multiple endocrine neoplasia type 1 gene, inhibits the commitment of multipotential mesenchymal stem cells into the osteoblast lineage. *J. Biol. Chem.* **278,** 21058–21069
20. Sowa, H., Kaji, H., Hendy, G. N., Canaff, L., Komori, T., Sugimoto, T., and Chihara, K. (2004) Menin is required for bone morphogenetic protein 2- and transforming growth factor β-regulated osteoblastic differentiation through interaction with Smads and Runx2. *J. Biol. Chem.* **279,** 40267–40275
21. Kaji, H., Canaff, L., Lebrun, J.-J., Goltzman, D., and Hendy, G. N. (2001) Inactivation of menin, a Smad3-interacting protein, blocks transforming growth factor type β signaling. *Proc. Natl. Acad. Sci. U.S.A.* **98,** 3837–3842
22. Hendy, G. N., Kaji, H., and Canaff, L. (2009) Role of menin in bone development. *Adv. Exp. Med. Biol.* **668,** 37–50
23. Zhang, M., Xuan, S., Bouxsein, M. L., von Stechow, D., Akeno, N., Faugere, M. C., Malluche, H., Zhao, G., Rosen, C. J., Efstratiadis, A., and Clemens, T. L. (2002) Osteoblast-specific knockout of the insulin-like growth factor (IGF) receptor gene reveals an essential role of IGF signaling in bone matrix mineralization. *J. Biol. Chem.* **277,** 44005–44012
24. Rossert, J., Eberspaecher, H., and de Crombrugghe, B. (1995) Separate cis-acting DNA elements of the mouse pro-α1(I) collagen promoter direct expression of reporter genes to different type I collagen-producing cells in transgenic mice. *J. Cell Biol.* **129,** 1421–1432
25. Canaff, L., Vanbellinghen, J. F., Kanazawa, I., Kwak, H., Garfield, N., Vautour, L., and Hendy, G. N. (2012) Menin missense mutants encoded by the *MEN1* gene that are targeted to the proteasome: restoration of expression and activity by CHIP siRNA. *J. Clin. Endocrinol. Metab.* **97,** E282–E291
26. Bouxsein, M. L., Boyd, S. K., Christiansen, B. A., Guldberg, R. E., Jepsen, K. J., and Müller, R. (2010) Guidelines of assessment of bone microstructure in rodents using micro-computed tomography. *J. Bone Miner. Res.* **25,** 1468–1486
27. Marulanda, J., Gao, C., Roman, H., Henderson, J. E., and Murshed, M. (2013) Prevention of arterial calcification corrects the low bone mass phenotype in MOP-deficient mice. *Bone* **57,** 499–508
28. Dempster, D. W., Compston, J. E., Drezner, M. K., Glorieux, F. H., Kanis, J. A., Malluche, H., Meunier, P. J., Ott, S. M., Recker, R. R., and Parfitt, A. M. (2013) Standardized nomenclature, symbols, and units for bone histomorphometry: a 2012 update of the report of the ASBMR histomorphometry nomenclature committee. *J. Bone Miner. Res.* **28,** 2–17
29. Richard, C., Huo, R., Samadfam, R., Bolivar, I., Miao, D., Brown, E. M., Hendy, G. N., and Goltzman, D. (2010) The calcium-sensing receptor and 25-hydroxyvitamin D-1α-hydroxylase interact to modulate skeletal growth and bone turnover. *J. Bone Miner. Res.* **25,** 1627–1636
30. Boraschi-Diaz, I., and Komarova, S. V. (2014) The protocol for the isolation and cryopreservation of osteoclast precursors from mouse bone marrow and spleen. *Cytotechnology* 10.1007/s10616-014-9759-3
31. Manolson, M. F., Yu, H., Chen, W., Yao, Y., Li, K., Lees, R. L., and Heersche, J. N. (2003) The a3 isoform of the 100-kDA V-ATPase subunit is highly but differentially expressed in large (≥10 nuclei) and small (≤5 nuclei) osteoclasts. *J. Biol. Chem.* **278,** 49271–49278
32. Rafiei, S., and Komarova, S. V. (2013) Molecular signaling pathways mediating osteoclastogenesis induced by prostate cancer cells. *BMC Cancer* **13,** 605
33. Murshed, M., Harmey, D., Millán, J. L., McKee, M. D., and Karsenty, G. (2005) Unique coexpression in osteoblasts of broadly expressed genes accounts for the spatial restriction of ECM mineralization to bone. *Genes Dev.* **19,** 1093–1104
34. Bakker, A. D., and Klein-Nulend, J. (2012) Osteoblast isolation from murine calvaria and long bones. *Methods Mol. Biol.* **816,** 19–29
35. Riddle, R. C., Diegel, C. R., Leslie, J. M., Van Koevering, K. K., Faugere, M.-C., Clemens, T. L., and Williams, B. O. (2013) Lrp5 and Lrp6 exert overlapping functions in osteoblasts during postnatal bone acquisition. *PLoS ONE* **8,** e63323
36. Aziz, A., Miyake, T., Engleka, K. A., Epstein, J. A., and McDermott, J. C. (2009) Menin expression modulates mesenchymal cell commitment to the myogenic and osteogenic lineages. *Dev. Biol.* **332,** 116–130
37. Engleka, K. A., Wu, M., Zhang, M., Antonucci, N. B., and Epstein, J. A. (2007) Menin is required in cranial neural crest for palatogenesis and perinatal viability. *Dev. Biol.* **311,** 524–537
38. Suda, T., Takahashi, N., Udagawa, N., Jimi, E., Gillespie, M. T., and Martin, T. J. (1999) Modulation of osteoclast differentiation and function by the new members of the tumor necrosis factor receptor and ligand families. *Endocr. Rev.* **20,** 345–357
39. Trouvin, A. P., and Goëb, V. (2010) Receptor activator of nuclear factor-kB ligand and osteoprotegerin: maintaining the balance to prevent bone loss. *Clin. Interv. Aging* **5,** 345–354
40. Martin, T. J., and Sims, N. A. (2005) Osteoclast-derived activity in the coupling of bone formation to resorption. *Trends Mol. Med.* **11,** 76–81
41. Haÿ, E., Lemonnier, J., Fromigué, O., and Marie, P. J. (2001) Bone morphogenetic protein-2 promotes apoptosis through a Smad-independent, protein kinase C-dependent signaling pathway, *J. Biol. Chem.* **276,** 29028–29036